Inkjet Printing

How to cite:
International Edition: doi.org/10.1002/anie.202200166
German Edition: doi.org/10.1002/ange.202200166

Challenges, Prospects, and Emerging Applications of Inkjet-Printed Electronics: A Chemist's Point of View

*Justin Lemarchand, Nathalie Bridonneau, Nicolas Battaglini, Florent Carn, Giorgio Mattana, Benoit Piro, Samia Zrig, and Vincent Noël**

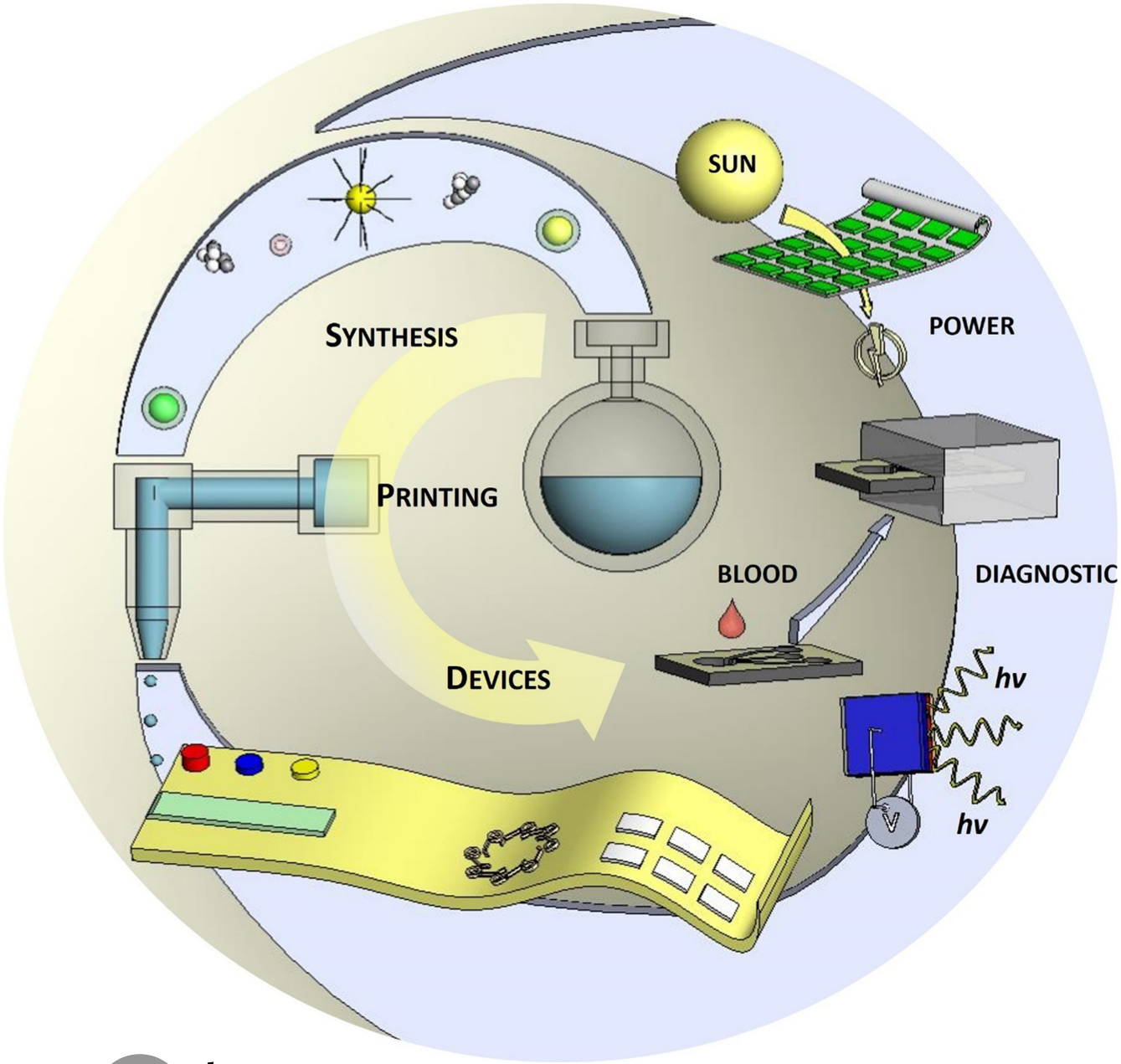

Abstract: Driven by the development of new functional inks, inkjet-printed electronics has achieved several milestones upon moving from the integration of simple electronic elements (e.g., temperature and pressure sensors, RFID antennas, etc.) to high-tech applications (e.g. in optoelectronics, energy storage and harvesting, medical diagnosis). Currently, inkjet printing techniques are limited by spatial resolution higher than several micrometers, which sets a red-hibitorythreshold for miniaturization and for many applications that require the controlled organization of constituents at the nanometer scale. In this Review, we present the physico-chemical concepts and the equipment constraints underpinning the resolution limit of inkjet printing and describe the contributions from molecular, supramolecular, and nanomaterials-based approaches for their circumvention. Based on these considerations, we propose future trajectories for improving inkjet-printing resolution that will be driven and supported by breakthroughs coming from chemistry. Please check all text carefully as extensive language polishing was necessary. Title ok? Yes

1. Introduction

Developed in the 1970s, inkjet printing experienced a first revolution in the early 2000s with the onset of printed electronics. Its ability to operate at ambient conditions and its low level of material waste lead to fabrication costs that are always competitive compared to that of manufacturing processes based on silicon-based technologies, gas- and liquid-phase deposition processes (CVD, electrodeposition, and spin-coating. These advantages have been successfully exploited by the electronics industry as a relatively simple means to increase the functionality of objects without significantly impacting their production costs. In parallel to the development of printed electronics, tremendous progress have been made in nanoscience in general and nano-chemistry in particular. Many ink formulations based on nanoparticles are currently available and innovations in this field are continuous, as underlined by recent reviews (on carbon materials such as graphene[1,2] and carbon nanotubes,[3,4] quantum dots for printed QLEDS,[5,6] inks based on Au[7,8] and Ag[9–14] nanoparticles and biomolecules[15,16]).

Thanks to these new generations of functional inks, printed electronics has reached several milestones upon moving from the integration of simple electronic elements (e.g., temperature and pressure sensors, RFID antennas, etc.) to high-tech application fields. The past twenty years have seen breakthroughs in several major technological fields such as flexible and organic electronics,[17–20] optoelectronics,[21] and energy storage and harvesting[22] as well as medical diagnosis (disposable analytical tests),[23,24] recently boosted by the COVID-19 crisis. The benefits of printing methods in these fields of application are extensive and well-founded. They are, however, only the basis for the further expansion of printed electronics applications. Indeed, printing methods may potentially reach another major milestone in the years to come, provided that two main topics are addressed: 1) the manufacturing of full-printed devices and 2) the printing of patterns showing enhanced properties thanks to the nanoscale organization of their constituents.

The use of exclusively printing steps makes it possible to simplify the design of production lines; this is the main driving force for the development of full printing fabrication processes. However, it requires a strong effort to improve the minimum size of the patterns that can be currently printed. A first general consideration for resolution improvement is that decreasing the dimensions of the printed components makes it possible to increase the density of functions. A more specific implication of the resolution limit arises when the device efficiency directly depends on the system dimensions. For example, the output signal (drain current) of field-effect transistors is inversely proportional to the distance between the source and drain electrodes. Any decrease of this gap leads to an increase of the magnitude of the output signal (keeping the same biasing voltages). To date, submicron-resolution printing is sought for most applications in (opto)electronics and energy production and storage devices, as highlighted in recent topic-related reviews.[25–29]

As previously mentioned, recent developments in nano-chemistry have led to the creation of functional nanoparticle-based inks that act as the basis for a new generation of printed devices, especially in the bio- and opto-electronics fields. However, to take full advantage of properties arising from the nanoscale, at least one dimension of the system must be below the characteristic length associated with the property that is being considered, e.g. thermal diffusion length, thickness of the diffusion layer, wavelength of electromagnetic radiation. An example of this principle concerns the realization of enzymatic cascade reactions, which requires the enzymes to be co-localized at a maximum distance comparable to the diffusion layer thickness, i.e. from 100 nm to 1 μm. Another example is represented by plasmonic structures such as localized surface plasmon resonance (LSPR) devices that require nanostructures separated by a gap smaller than the light wavelength in order to produce enhanced spectroscopic signatures of elements arranged in between. For such an application, the

[*] J. Lemarchand, Dr. N. Battaglini, Dr. G. Mattana, Dr. B. Piro, Dr. S. Zrig, Dr. V. Noël
Université de Paris, CNRS, ITODYS
75013 Paris (France)
E-mail: vincent.noel@u-paris.fr
Dr. N. Bridonneau
ICMMO, CNRS, Université Paris Saclay UMR 8182
91405 Orsay (France)
Dr. F. Carn
Université de Paris, Laboratoire Matière et Systèmes Complexes
CNRS, UMR 7057, 75013 Paris (France)

characteristic dimensions of the pattern must be below 100 nm.

All the high-added-value applications considered here underline the need to control materials deposition and organization on a large scale, which is sometimes over three

Justin Lemarchand received his MSc degree (2019) in nanochemistry, materials, and surfaces from the University of Paris Diderot. He is currently a PhD candidate at ITDOYS laboratory at the University of Paris. His current research, conducted, under the supervision of Professor Vincent Noël, is focused on inkjet-printed metallic micropatterns for electroanalytical applications.

Nathalie Bridonneau received her PhD in inorganic chemistry in 2013 under the supervision of Dr. V. Marvaud at Sorbonne University (Paris, France), where she investigated multimetallic photomagnetic molecules. As a postdoctoral researcher, she worked for several years on the synthesis of gold nanoparticles and their interaction with polymers as well as their deposition by inkjet process. In 2019 she was appointed CNRS researcher in the Inorganic Chemistry team of the ICMMO laboratory of the University of Paris Saclay. Her current research focuses on the design of magnetic molecules (single-molecule magnets and qubits) whose properties are photo- and electroswitchable.

Nicolas Battaglini is an associate professor in the chemistry department (ITODYS lab, team Bioelectronics and Smart Surfaces) at Université de Paris (France). He obtained his PhD degree in the physics of materials from Aix-Marseille Université (France) in 2004, followed by a postdoctoral stay at Université Paris Diderot (France). His current research activities focus on electronic properties of assemblies of functional organic and graphene-based materials for printed electronics applications.

Florent Carn is an associate professor at the University of Paris and a researcher at the Laboratoire Matière et Systèmes Complexes. He obtained a PhD in the physical chemistry of condensed matter from the University of Bordeaux in 2006. He was a postdoctoral fellow at the Collège de France before taking up his current position in 2008. His research focuses on the study of assembly/disassembly processes of nano-objects in complex media.

Giorgio Mattana received his MSc degree in electronic engineering in 2008 and his PhD degree in electronic and computer science engineering in 2011 from the University of Cagliari (Italy). He joined the Ecole Polytechnique Fédérale de Lausanne (Switzerland) in 2011 as a postdoctoral researcher, then he joined the ITODYS Laboratory, Université de Paris (France) as an associate rrofessor in 2015. His research interests include printed and organic electronics, in particular for the fabrication of chemical and biological sensors.

Benoît Piro received his MSc in 1995 (University of Poitiers, France) and his PhD in 1998 (Université Paris 7, Denis Diderot, France) before he joined the laboratory ITODYS in 1998. He developed materials for lithium batteries and worked on electrochemical biosensors. Since 2010, he has developed organic electronic devices for sensing, including organic field effect transistors and more precisely electrolyte-gated OFETs and graphene FETs, applicable to aqueous media with potential applications in the medical and environmental fields. Since 2016, he has also focused on printed organics electronics, not only for chemical but also for physical sensing.

Samia ZRIG has completed her PhD in a cooperation program between Université Pierre et Marie Curie (France) and Kathioleke Universiteit Leuven (Belgium) on the synthesis of chiral oligothiophenes. During her postdoctoral training, she worked on new polyporphyrinic semiconductors (University of Pennsylvania, USA), and organometallic helicenes (Université de Rennes 1, France). In 2010, she was appointed associate professor at the Université de Paris (France) to work on the elaboration of supramolecular assemblies of organic semiconductors for printed electronics.

Vincent Noël has been a full professor at the University of Paris and a researcher at the ITODYS Laboratory since 2018. After a completing a PhD in electrochemistry (Université de Cergy, France), he was a postdoctoral fellow at the Commissariat à l'Energie atomique (Saclay, France). In 2004, he joined the ITODYS Lab to develop surface-functionalization strategies dedicated to the realization of electrochemical biosensors. Currently, his research focuses on the use of inkjet printing to fabricate ultrasensitive analytical devices (organic transistors, electrochemical biosensors, development of new sorting paradigm).

orders of magnitude, i.e. from 100 nm to 100 μm. The current limitations of printing techniques do not allow spatial resolution below the micrometer scale. Nevertheless, the field is extremely dynamic and new methods of improving printing resolution have recently been explored. Two main approaches can be identified, namely top-down and bottom-up strategies. In the top-down approach, the resolution issue is addressed by implementing physical or chemical nano- or micro-structuration on the substrate to be printed, thus allowing control of the ink-wetting processes. In parallel, continuous advances made in the field of nano- and supramolecular chemistry are used directly to improve printing resolution through a bottom-up approach. Here, ink constituents are designed such that they organize in multi-scale patterns, including nanostructures.

To strengthen and boost the research field at the junction of inkjet printing and high-tech applications such as optoelectronics and (bio)detection, but also to identify potential future breakthroughs, it is interesting to assess the methods of micro- and nanostructuring through inkjet printing and answer the following questions: What are the current methodologies to improve the resolution of printed patterns? To what extent can advances in surface chemistry, Nanochemistry, and supramolecular chemistry be integrated into innovative printing strategies? Following a presentation of the physico-chemical concepts and the equipment constraints underpinning the resolution limit of the inkjet printing method (Section 2), we will describe the molecular, supramolecular, and nanomaterial-based approaches to overcome these constraints (Section 3). The complementary approach, consisting of tuning the pattern features by micro-structuring the substrate before printing, will be also analyzed in detail (Section 4). Finally, current methods that combine advances from both the bottom-up and top-down approaches, made possible by recent progress in related scientific fields, are described and used as the basis to propose future trajectories for inkjet-printing (Section 5).

2. Underpinning Concepts of Printing Processes: From Equipment to the Physics of Sessile Droplets

In this section we review the elements needed to understand the current issues related to all-printed devices. Printing with multiple inks without denaturing them and obtaining optimal resolution for each of them requires the choice of the right technique as well as the understanding of the physics underlying both the transfer processes of the materials (from the ink reservoir to the on-substrate spreading) and the ink-drying step. The most important factors affecting the spatial resolution of printed layouts (namely, equipment geometry, printability, wettability, and coalescence of droplets) will be considered.

2.1. Overview of Printing Technologies

The most common printing technologies are contact printing methods, in which an image carrier comes into physical contact with the substrate. These techniques include offset printing, flexography, gravure, and screen printing. Contact printing technologies have been thoroughly reviewed in other excellent papers.[30–32] The inks for contact printing techniques must be of much higher viscosity than the inks utilized for other technologies (see Table 1), since in the former, inks are subjected to much more intense mechanical stresses (in particular shear rates).[33] The need for high viscosity is usually satisfied with ink formulations characterized by large proportions of solid content (>60 wt. %), thickeners, and active materials.[34–36] These formulations are not ideal for the printing of biomolecule- and nanostructure-based inks, which typically require very dilute conditions.[37,38]

2.2. Inkjet Printing Technologies

Inkjet printing is a fully digital (maskless) and non-contact technique. Inkjet printing relies on the generation of droplets of liquid ink ejected from nozzles of a printing head toward a substrate, where they accumulate and form a given pattern. There are two categories of inkjet printing technologies: those based on a continuous inkjet (CIJ), and those based on the discontinuous ejection of the ink in the form of individual drops, i.e. the drop on demand (DOD) technology. Within these categories, different mechanisms are used to eject the droplets: thermal actuation (where a bubble of gas generated by heating expands in the reservoir and ejects the ink from a nozzle), piezo actuation (in which the deformation of a piezoelectric actuator generates pressure waves within the ink reservoir, which spread and expel droplets through a nozzle), acoustic actuation (where an acoustic wave is focused at the surface of the ink to expel a droplet), and electrohydrodynamic actuation (EHD) (where the droplet ejection is assisted by the application of a strong

Table 1: Requirements and characteristics of contact printing technologies.[39]

Technique	Ink viscosity [cP]	Lateral resolution [μm]	Thickness [μm]	Throughput [$m^2 s^{-1}$]
Screen-printing	1000–50 000	30–100	30–1000	2–3
Gravure	20–500	5–20	1–10	60
Offset	40 000–100 000	10–50	0.5–2.5	5–30
Flexography	50–500	80	1–10	10
Electro-hydrodynamic actuation (EHD)	3–4000	2–50	<0.5	$<10^{-4}$
Continuous jet	1–30	100–200	<0.5	10^{-3}–0.5
Inkjet-printing	1–30	20–50	<0.5	10^{-3}–0.5

electric field). These techniques, and particularly the DOD methods, are restricted to inks of limited viscosity and surface tension ranges compared to the inks used for offset, flexography, or screen printing. In the field of printed electronics, the piezo and electrodynamic actuation mechanisms are nearly always used; they are described more in detail in the following section.

2.2.1. Electrohydrodynamic Actuation

Readers particularly interested in electrohydrodynamic inkjet printing can refer to several dedicated reviews including ref. [40]. Briefly, EHD is a technique first reported in 2007[41] which theoretically offers better printing resolution than conventional continuous inkjet or DOD printing. For this reason, it is applied in the printed electronics domain, where integration of printed components of nanometer dimensions is critical. As discussed in the previous section, the lateral resolution of all inkjet techniques depends (among other parameters) on the size of the droplets, which is itself limited by the size of the nozzle. The issue is then to reduce the nozzle size, but this approach considerably increases the risks of clogging and limits also the viscosity and surface tension ranges of usable inks. Electrohydrodynamic ejection overcomes these difficulties because the diameter of the droplets can be smaller than the nozzle diameter. This technique uses an electric field to create, accelerate, and guide the droplets towards the substrate (Figure 1).[42–49] In EHD, therefore, the ink is pulled out from the nozzle, while in conventional inkjet printing it is pushed out of it instead. Rogers et al. pushed the electrohydrodynamic printing technique to its limits and demonstrated droplet sizes lower than 1 μm and printed lines of 2–3 μm in width.[41] Since the lateral resolution of EHD is high, it represents an efficient technique to finely pattern large-area substrates. The main limitation of this approach is that in order for the drop to be emitted, the ink must be electrically polarizable (separation of charges under the applied electric field).

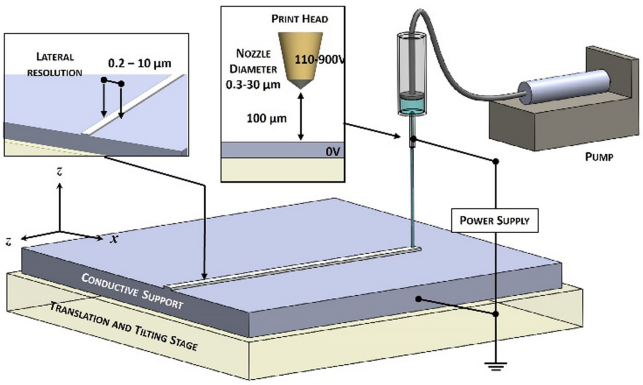

Figure 1. EHD complete setup, comprising a fixed nozzle, a syringe pump, and an x-y-z plate. Adapted from Ref. [41].

2.2.2. Piezoelectric Actuation

In inkjet printing relying on piezoelectric actuation, the pressure increase inside the ejection chamber is controlled by a small actuator which is fixed onto the reservoir wall, which deforms upon application of a voltage pulse (Figure 2). This results in a change of the chamber volume, which corresponds to an increase of internal pressure, pushing the ink through the nozzle. If the deformation amplitude is in the micrometer range, the area of the actuator must be relatively large to be able to create a drop of significant volume (several pL). The voltage waveform applied to the piezo actuator can be composed of several segments with different slopes, amplitudes, and durations, which allows fine control of the quality (shape, volume, and speed) of the ink droplets. Typically, with the smallest usable nozzle diameter (ca. 10 μm), droplets have a volume of about 1 pL.

In contrast to thermal jetting, complex inks such as polymers, suspensions, and even thermally fragile biomolecules can be printed by piezoelectric actuation without restriction. For this reason, piezo actuation is preferred for research and development printers. There is also no restriction on the type of solvent (aqueous, aliphatic, or aromatic), as cartridges can be easily adapted—another reason why piezoelectric-based printers are more often used in R&D rather than thermal jetting printers (such as the Jetlab systems[50] from MicroFab, the Dimatix material printer from Fujifilm,[51] Ceradrop[52] from MGI, and even the Autodrop printing systems from Microdrop[53]).

2.3. Resolution Limit Depends on Equipment Geometry

Piezoelectric actuation produces droplets between 10 and 60 μm in diameter, a parameter directly related to the diameter of the ejection nozzle. For inkjet printing, this diameter is the first parameter that limits the printing resolution in a particular dimension. To ensure well-defined droplets, inks must fulfill specific rheological requirements.

Printability (i.e., the compatibility between a given ink and the printer chosen for its deposition) can be assessed by calculating the inverse Ohnesorge number Z,[55] which is defined as the ratio of the Reynolds number (Re) and the square root of the Weber number (We), which are calculated from γ the ink surface tension, ρ the density, η the dynamic viscosity, v the jet velocity, and d the nozzle diameter [Eqs. (1)–(3)].

$$Re = \frac{\rho v d}{\eta} \tag{1}$$

$$We = \frac{\rho v^2 d}{\gamma} \tag{2}$$

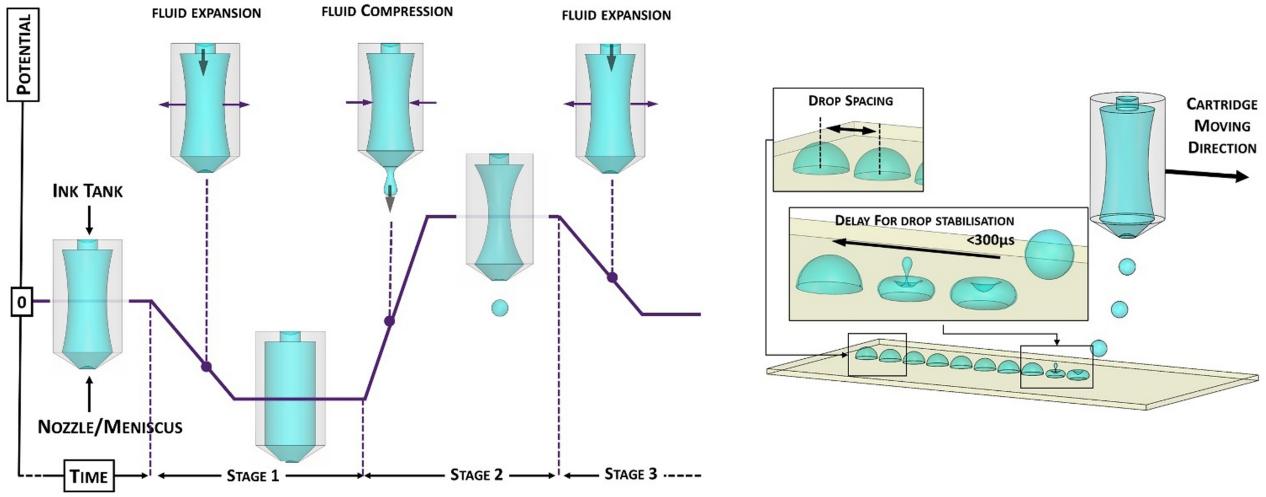

Figure 2. Left: Inkjet printing based on piezoelectric actuation. The pressure inside the ejection chamber in the nozzle is controlled by an actuator having a bipolar waveform with programmed sequences; a droplet and then the reservoir is refilled. The waveform (i.e. the typical time evolution of the voltage applied to each nozzle of the inkjet printer when a drop is ejected) can be divided into three parts, each o which can be controlled in terms of amplitude, duration, and slew-rate: Stage 1. A negative voltage causes an expansion of the nozzle's reservoir and determines the volume of ink drawn inside the reservoir. Stage 2. A positive voltage causes a compression of the nozzle's reservoir and determines the form and the speed of the ejected drop. Stage 3. The voltage is slowly brought back to zero, whichallows the gradual return of the walls to their initial position. Sometimes this last stage is decomposed into two negative-slope substages with a constant voltage applied in between in order to avoid the formation of satellite droplets. Right: DOD printing pattern processes. Upon jetting, drops impact the substrate and reach a first stationary dome-shape after a few hundreds of µs. Printer head displacement rate and overall waveform cycle duration control the drop spacing on the substrate.[54]

$$Z = \frac{Re}{\sqrt{We}} = \frac{\sqrt{\gamma \rho d}}{\eta} \tag{3}$$

For the formation of a single stable droplet, the ink must have a Z value in the range of $1 < Z < 10$. For $Z < 1$, the ink is too viscous and drop ejection from the nozzle is prevented; on the other hand, for $Z > 10$, satellite droplets are formed. This is applicable to Newtonian fluids. For nonlinear fluids, the printability window can be enlarged to Z values ranging from 1 to several tens, without the formation of satellite drops. Improving printing resolution by decreasing the nozzle diameter decrease is limited by the ability to form well-defined and independent droplets.

2.4. Basics of Wettability Processes

The surface energy of the substrate as well as its topography strongly impact the behaviorof a droplet freely lying on its surface (sessile droplet).[56] Both the static characteristics and the dynamics of evaporation of a sessile droplet determine the final distribution of the ink components. In this section we introduce the theoretical background required to understand the roleof capillary forces in the inkjet printing process.

As shown in Figure 3a, when a liquid is deposited on a solid surface (i.e. sessile droplet), a geometrical angle, measured from the liquid–gas interface to the liquid–solid interface, is usually observed when the droplet reaches its equilibrium . This angle is denoted θ_{Eq} and is called the static contact angle. The small droplets deposited by inkjet printing are spherical due to the negligible influence of

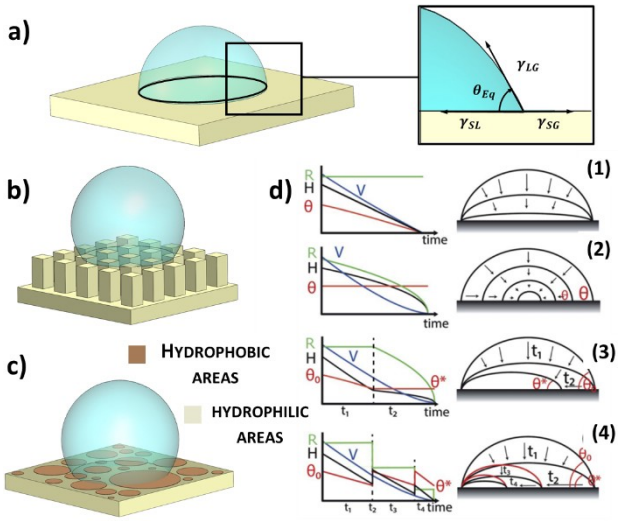

Figure 3. a) Schematic representation of a sessile droplet lying on a substrate with a contact angle defined by Equation (4). Sessile droplet on a physically textured substrate (b) and on a chemically textured substrate (c). d) Schemes of the four possible evaporation modes of a surface nanodroplet (or a surface nanobubble): (1) CCR mode. (2) CCA mode. (3) Stick-slide mode. (4) Jumping mode. R: drop radius, V: drop volume, H: drop height, adapted from Ref. [57].

gravity and the shape is determined by the contact angle. θ_{Eq} is defined macroscopically, on a scale greater than that of surface roughness and long-range intermolecular forces. The intersection line where the three phases (i.e. liquid, solid, gas) meet is called the triple line or the contact line. When the contact line is in motion, the terms "dynamic contact

angle" and "dynamic contact line" are used. Depending on the value of θ_{Eq} one can distinguish between non-wetting ($\theta_{Eq}=180°$), partial wetting ($0°<\theta_{Eq}<180°$), and total wetting ($\theta_{Eq}=0°$) situations. The different wetting states can also be distinguished by considering the equilibrium spreading coefficient, S_{Eq}, which represents the surface free energy γ_{SG} relative to its value for total wetting [Eq. (4)]:

$$S_{Eq} = \gamma_{SG} - (\gamma_{SL} + \gamma_{LG}) = \gamma_{LG}(cos\theta_{Eq} - 1) \tag{4a}$$

with

$$\gamma_{SG} = \gamma_{SL} + \gamma_{LG} \tag{4b}$$

when ($\theta_{Eq}=0°$) (i.e. total wetting). For non-wetting or partial wetting situations, the static contact angle may take different values. For example, if the solid surface on which the drop is placed is tilted from the horizontal, the static contact angle at the front of the drop is usually larger than the contact angle at the rear. This phenomenon is referred to as as contact angle hysteresis. The possible values of the static contact angle are between two limits. The upper limit is called the advancing contact angle and corresponds to the angle above which the triple line moves out. The lower limit, called the receding contact angle, is the angle below which the contact line will retract back. For a sessile droplet on a rigid, flat, and chemically homogeneous substrate, a unique value is expected for θ_{Eq}. In 1805, Young proposed an equation linking this value of θ_{Eq} and the surface tension at the three interfaces (solid–liquid, liquid–gas, and solid–gas) that need to be considered as follows [Eq. (5)].

$$\gamma_{SG} - \gamma_{SL} - \gamma_{LG} = 0 \tag{5}$$

This equation can be interpreted simply as a force equilibrium on the contact line, since surface tension corresponds to energy per unit area, equivalent to force per unit length acting on the contact line. This relation corresponding to a situation where the surface energy is minimized could be also retrieved using energetic arguments at thermodynamic equilibrium where the system is in mechanical (i.e. force equilibrium), thermal (i.e. same temperature everywhere), and chemical equilibrium (i.e. same chemical potential everywhere) at the same time.

In 1936, Wenzel extended the work of Young by considering a liquid that fits perfectly on a rough surface (Figure 3b). In this case, according to the Wenzel equation [Eq. (6)], the apparent contact angle θ_w differs from the angle of equilibrium.

$$\cos\theta_W = r\cos\theta_{Eq} \tag{6}$$

The factor r is the ratio of the real to the projected area covered by the drop. If r is greater than unity, the roughness amplifies the hydrophobic character of the surface. In 1944, Cassie and Baxter considered the case of a flat surface with chemical heterogeneities such that the spreading coefficient varies locally (Figure 3c). They assumed that if the chemical heterogeneities are weak, Young's equation should hold, provided that the equilibrium spreading coefficient is replaced by its averaged value $\bar{S}$, leading to the so-called Cassie–Baxter equation [Eq. (7)].

$$\gamma_{LG}(cos\theta_{CB} - 1) = \bar{S} \tag{7}$$

These equations also consider that wettability properties are exclusively dependent on the liquid/solid contact area.

The behavior of liquids on solid surfaces presenting a chemical (alternation of hydrophilic and hydrophobic zones) or physical texture (grooves, dots, etc.) has been studied for a long time, both from experimental and theoretical points of view.[57,58] It appears that the Wenzel and Cassies–Baxter equations fail to describe all the contact angle dynamics upon changes in the drop volume.

This is the situation found in inkjet printing when the liquid phase of the ink evaporates. Although this subject remains open to discussion, it is recognized that the mechanism of evaporation of a droplet depends to a large extent on the dynamics of the contact line. According to Parsa et al., the evaporation of sessile droplets can occur following different modes described as follows.[58]

Constant contact radius (CCR) mode. Here, the contact line (CL) is pinned for most of the evaporation process, whereas the contact angle decreases with time (Figure 3d (1)). This mode of evaporation often occurs on rough substrates and allows uniform deposits or coffee rings to form. The formation of either of these patterns is governed by the flow field (i.e. capillary flow, Marangoni flow) within the drying droplet. For a given set of experimental conditions, the evaporation rate of the solvent at the periphery of a droplet can be higher than at its center. These dynamics results in an outward solvent flow and triggers the capillary flow of the solute particles, leading to the accumulation of particles at the edge of the droplet and a ring-like structure. This pattern is referred to as a "coffee ring".[59]

Constant contact angle (CCA) mode. Here, the contact angle remains unchanged during the evaporation process, whereas the wetted contact area shrinks (Figure 3d (2)). This mode of evaporation occurs typically with smooth hydrophobic substrates and favors the formation of dot-like patterns. The Wenzel and Cassie–Baxter models accurately describe this type of dynamics.

Stick-slip (CL) mode. Here, the CL is pinned (CCR mode) at the beginning of the evaporation process and a flow is created from the center of the droplet to its edge to supply the liquid to the edge (Figure 3d (3)). This flow transports particlesto the edge and deposits them near the CL. As the droplet volume decreases by evaporation, the contact angle decreases and creates an inward unbalanced force (depinning force) that acts on the contact line. When the contact angle becomes less than the receding contact angle (i.e. the angle at which the contact line starts to recede), the contact line slips and moves quickly toward the center until it becomes pinned again. This mode of evaporation generates multi-ring pattern features.

Jumping mode. Here, the mode of evaporation changes (Figure 3d (4)). For instance, dot-like patterns surrounded

by multi-ring pattern can be obtained through the combination of CCA mode and CCR mode on hydrophilic substrates with low particle concentrations, regardless of the particle/substrate interaction.[60]

The aforementioned phenomena are quite complex and can be modeled using two different approaches. According to thermodynamics, the dynamics of the contact line is controlled by the height of an energy barrier that the system must overcome to reach a lower-energy equilibrium position, whereby the barrier height depends on local topological or chemical heterogeneity.[61,62] However, this macroscopic view is in contrast with a microscopic model, which can be used to describe evaporation processes for which the Wenzel and Cassie–Baxter equations are not verified.[61–66] This model is based on a mechanical point of view considering the forces exerted at the liquid/gas/solid triple point, i.e. along the CL (where the balance of forces holds).[67] In the case of the thermodynamic model, the contact line moves when the energy gain is greater than the energy barrier. In agreement with the microscopic/mechanical model, the contact line slips only when the driving force is larger than the maximum force that the solid substrate can provide (balance of forces). Because of these divergent interpretations, the field still requires basic research efforts to achieve unified modeling.[65] It should be noted, however, that in both models the dynamics of the contact line are, to a large extent, controlled by the texture of the substrate and that it is possible to take advantage of this to control both the initial size of the ink droplet and its drying dynamics.

2.5. Modeling: From Sessile Droplets to Drop-on-Demand Systems

When a droplet consisting of a particle suspension is deposited on a solid substrate and dries in open air, the resulting solid deposits form uniform disc patterns, coffee rings, stick-slip patterns, fingering patterns, dot-like patterns, or a combination of these different patterns. At the present time, overwhelmingly uniform deposit forms have been desired in the field of inkjet printing, but several recent studies have shown the value of targeting non-uniform deposits like coffee rings. Although the mechanisms behind the formation of specific patterns have been studied for many years, they are not yet fully understood.[58] Indeed, distinguishing the modes of evaporation on the basis of contact line dynamics and contact angle evolution does not make it possible to anticipate the formation of a particular type of deposit (as described in the previous section). Indeed, it appears that different types of deposits can be obtained for the same evaporation mode and that reciprocally the same type of deposit can be obtained with different evaporation modes. This is due to the contribution of other parameters including evaporation kinetics, inner flow field, interfacial interactions, and particle–particle interactions. These factors may be manipulated individually by changing the solute (size, concentration, surface chemistry), the substrate (temperature, wettability), the atmospheric conditions (relative humidity, temperature), the solvent (pH, ionic strength), and the presence of surfactants. It is difficult to discuss the role of each individual parameter in determining the final structure of the deposit because, despite the large number of studies carried out to date, too few studies clearly mention all the characteristics of the systems studied, which limits comparisons. Moreover, while many in-depth studies focus on the drying dynamics of colloidal sessile droplets for inkjet applications,[68] to date, only few experiments have been conducted under real conditions in terms of the printing process (ambient conditions, drop volume),[69,70] ink formulation (dilute systems, organic solvents), and finally in terms of the substrate,[71,72] which is often quite rough, e.g. plastic foils or fibrous surfaces such as paper sheets and textiles.

Using sessile droplets as a model system to predict ink behavior and, consequently, printed pattern features (dimensions, sharp edges…) is often inaccurate. Indeed, unlike classical graphics printing, which is based on isolated drops to produce pixelated pictures, the elaboration of functional electronic devices (e.g. interconnection of conductive tracks) requires continuous patterns. In an inkjet printing system, the distance between the centers of two adjacent droplets, called the drop spacing, determines the amount of ink deposited by surface unit. A printed line results from the coalescence of individual printed drops, the process starting from droplet coalescence to the complete solidification of a stable line on the substrate. As summarized in Figure 4, it has been shown that the drop spacing significantly influences the morphology of the final printed line.

Starting from a dotted line, if the drops are printed with a separation greater than their diameter (Figure 4a), a

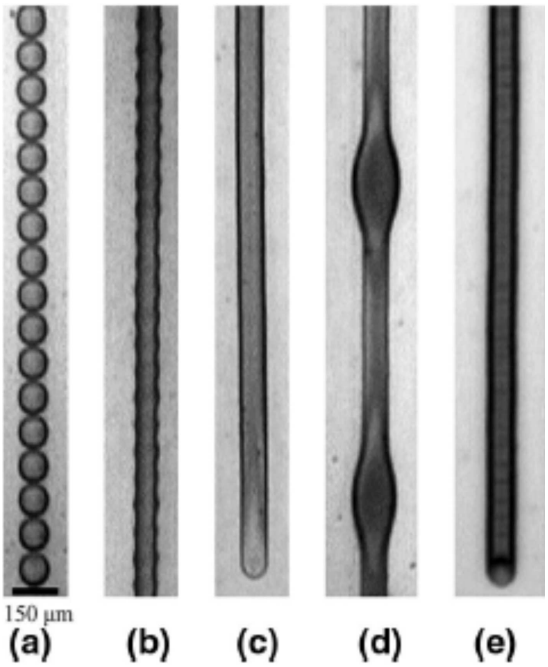

Figure 4. Morphology of inkjet-printed lines as a function of the drop spacing. Reprinted with permission from Ref. [73]. Copyright 2008, American Chemical Society.

decrease in the drop spacing leads to a merging of the drops to form "scalloped" lines (Figure 4b) until a straight uniform profile is reached (Figure 4c). A further decrease of the drop spacing increases their overlap, leading to bulging lines (Figure 4d). Finally, if the printing parameters are set in such a way that the drying time of a droplet is shorter than the ejection period of a single droplet, each droplet will dry individually, resulting in a "stacked coin" morphology (Figure 4e). In this situation, the line width is not impacted by the drop spacing, as each individual drop dries completely before the next droplet is deposited; the line thickness and morphology, however, are highly irregular. To print lines exhibiting uniform morphology, it is thus necessary for the droplets to coalesce in the liquid phase. Furthermore, it is essential to have sufficient contact angle hysteresis to prevent contact line recession when the droplets coalesce in order to minimize surface energy. Starting from these considerations, theoretical models have been developed that agree well with experimental results for a large variety of ink/substrate combinations in order to predict the width of the final printed track as a function of the drop spacing, drop diameter, and contact angle. Finally, a stability map could be established for predicting the morphology of the printed line as a function of ink properties, printing conditions, and ink/substrate interactions.[74,75]

2.6. Concluding Remarks

Contact printing methods are relevant for many applications. They have features which can hardly be matched by inkjet printing, especially in terms of writing throughput. However, inkjet printing still appears to be the most promising additive fabrication method since very small liquid volumes of dilute inks are required for deposition at precise locations with minimal surface contamination and ink waste.[76]

Even if inkjet printing fulfills most of the requirements for the printing of functional inks, especially those composed of nanomaterials or biomolecules, the main limitation concerns the minimal pattern size (spatial resolution). Assuming that a 10 pL droplet on a substrate has an ideal dome shape, its diameter is ca. 130 μm, which can be considered as the minimal dimension of any inkjet-printed pattern. However, droplet shape is also dependent on the capillary forces acting between ink, substrate, and atmosphere.

An obvious simple strategy to decrease droplet diameter would be to reduce droplet volume. Indeed, the relationship between nozzle diameter and droplet volume was established[77] and femtoliter droplets were obtained by reducing the nozzle diameter.[78] However, this approach is not as straightforward as it may seem. Indeed, the transformation of a thin cylinder of liquid flowing from a nozzle into single, spherical droplets occurs only if the process is energetically favorable, i.e. if the surface-to-volume ratio of said droplets is lower than the surface-to-volume ratio of the initial cylinder. This may not be the case for very small droplet volumes.[79] Moreover, smaller volume droplets typically require higher jet speed to ensure straight vertical trajectories,[80] but this also results in more intense splashing phenomena[81] which, in turn, compromise printing resolution.

A final aspect which should be considered is the precision of the printer's mechanical positioning stage which, for contemporary piezoelectric technology, is a few μm at best.[82] It is noteworthy that increasing the accuracy of equipment positioning down to the sub-micrometric scale would be countered by a significant decrease in the printing velocity. A trade-off is then necessary to find a good balance between resolution and throughput.

All these considerations make it unlikely that spatial resolution can be improved based purely on equipment or volumetric factors and justify approaches that depend instead on the substrate surface energy or topology, such as those described in the next sections.

3. Functional Nanomaterial-Based Inks for Emerging Applications

3.1. Functional Inks: State of the Art

Inkjet printing is particularly adapted for implementing functional nano-objects in a wide range of applications such as bio-analytical methods (sensor arrays for environmental monitoring, e-health), energy harvesting, and optoelectronics. The following applications require the deposition of well-defined printed nano/micropatterns under conditions that allow the ink to retain its functional properties.

3.1.1. Bio-active Inks

There is an increasing interest in inks that contain at least one element which is a biomolecule (proteins, nucleic acids, etc.).[23] To be suitable for inkjet printing, bio-inks obviously need to meet specific criteria in terms of viscosity and surface tension. These requirements necessitate the use of solvent mixtures and the addition of amphiphilic molecules such as surfactants. Bio-inks are water-based and, therefore, show low viscosity and high surface tension. Viscosity issues can be overcome by tuning the piezoelectric actuation waveform: current DOD equipment allows accurate printing of very low viscosity formulations. However, the surface tension issue remains and requires the addition of surfactants which can irreversibly unfold some biomolecules leading to a loss of their activity (catalysis, affinity, etc.).[83] Hence, the barrier to printing active biomolecules lies in the stability of the biomolecules themselves under stringent conditions, as well as in their capacity to maintain or to recover their native conformation. Basically, two main types of biomolecules are commonly employed: proteins[83,84] and nucleic acid sequences (note that inkjet printing of cells is not discussed here; readers interested in other application fields such as tissue repair will find exhaustive information in a recent high-quality review[23]). DNA and RNA are easy

to handle thanks to their resistance to heat and to their fast and reversible conformational change. Therefore, inkjet printing has been used for a long time to pattern DNA on substrates for bioanalytical applications.[85,86]

In order to develop stable bio-inks, proteins must be protected in a host matrix such as conductive polymers. Yun et al. used an aqueous bioelectrical ink containing PEDOT:PSS, glucose oxidase (GOD), and horseradish peroxidase (HRP), and they inkjet-printed a glucose biosensor on ITO-coated PET films.[87] More recently, an interesting entrapment strategy was developed in which enzymes were incorporated into porous materials such as metal–organic frameworks (MOFs). Hou et al. used a zeolitic imidazolate framework (ZIF-8) to immobilize flexible protein molecules (such as bovine serum albumin, BSA).[88] They showed that these enzyme–MOF composites can be successfully used for inkjet printing on various substrates. They applied this methodology to realize a *cytochrome C*–MOF composite, allowing the rapid detection of hydrogen peroxide in solution. As H_2O_2 is the enzymatic product of the broad class of oxidases, this printed biosensor may be applied for the specific detection of several analytes of interest, including glucose, lactate, and pyruvate.

Due to storage issues, the use of biomolecules can be a challenge for mass production in industrial processes. This problem was tackled by Tijero et al., who showed that the inkjet method can be used to make a UV-photoprintable ionogel-based microarray to efficiently store avidin biomolecules for more than 1 month at room temperature.[89] This method could be useful for the mass production and could be also applied to other proteins.

Bio-ink printing is in its early stages but clearly represents an expanding field of investigation owing both to the current need for portable and user-friendly bioanalytical tools and the variety of biomolecules that can be printed. Challenges still remain in the design, synthesis, and formulation of host matrices that can shield biomolecules both during the printing process and storage. Indeed, biomolecules could be irreversibly unfolded as a result of shear stresses during the drop ejection process.

3.1.2. Inks for Optoelectonics

Optoelectronics is a dynamic research and development field that has already benefitted from printing techniques, especially for the deposition of organic semiconductors in devices such as photodiodes and OLEDs. More recently, attention has been focused on quantum dots (QDs) and quantum rods (QRs) because of their enhanced optical and electrical properties. Such nanomaterials improve the efficiency of liquid crystal displays (LCDs) thanks to their optical properties (wide-ranging color tunability, high brightness, and narrow emission bandwidth). The spatial alignment of QDs and QRs must be precisely defined in order to show good optical efficiency. The accuracy of the inkjet printing technique to form precise QD patterns was first demonstrated in 2009 by Haverinen et al.[90,91] and then extended to printing on a wide variety of surfaces including photo-quality inkjet paper, cotton fabrics, PET films, and glass.[92–94] In 2020 Xuan et al. demonstrated the association of QDs with micro light-emitting diodes (μLEDs) for use in high-resolution and full-color printed μLED displays.[27]

However, even recent examples of quantum dot light-emitting diodes (QLEDs) are not efficient enough for use in commercial display applications.[5,94] This is in part due to the inkjet printing process itself, which has shortcomings such as low resolution and low deposit uniformity. The quality of printed QLEDs currently is limited by nonuniformities in droplet formation, wetting, and drying during inkjet printing. Yang et al. use a solvent mixture to provoke Marangoni flows that prevent coffee rings (Figure 5).

Array devices are printed at a resolution of 500 pixels inch?$^{-1}$ with a maximum luminance of ca. 3000 cd m^{-2}. More recently, to mitigate this issue, Zang et al. enhanced the emission yield by using hybrid displays.[95] They reported a full-color QD/OLED display from the stacking (either in parallel or in series) of a yellow QD-LED with a blue OLED, using an indium-zinc oxide intermediate connecting electrode. The inkjet-printed tandem LED can emit with a high brightness of 107 000 cd m^{-2}.

A photonic crystal is a regular arrangement of nanoparticles that gives rise to a specific optical signature. Inkjet printing is considered to be an adequate solution to pattern macroscopic surfaces with such optically active crystals, provided that a very uniform and thin (ideally a monolayer) deposit is achieved.[96–100] Liu et al. developed this approach using poly(styrenemethacrylic acid) colloidal inks that led to the fabrication of brilliant-color photonic devices.[96,97] Strong attention was devoted to the formulation of the ink in order to suppress the coffee-ring effect and to achieve thin and uniform deposition (see Section 3.2). Neterebskaia et al. also described the self-assembly of polystyrene spheres into photonic crystal arrangements and underlined that the printed pattern, drop spacing, and temperature regime of drop-drying have to be carefully chosen to obtain high-dimension photonic crystals.[98] They evaluated the close-packing of equal spheres of PSS by the Fourier method and showed a higher degree of ordering at the edge of the drop due to Marangoni flows. Another interesting system was

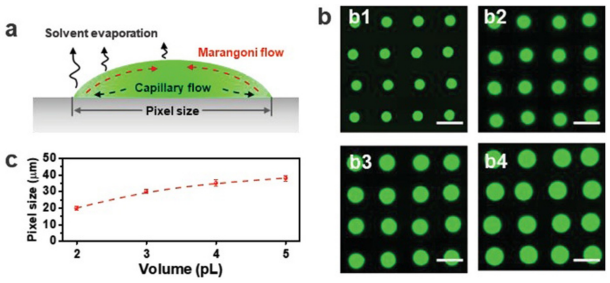

Figure 5. Printing of pixel arrays by the deposition of single inkjet droplets. a) Schematic illustration of the drying of printed pixels. b) Photoluminescence micrographs of pixels formed with droplet volumes from 2 pL (b1) to 5 pL (b4) at a constant density (scale bar: 50 μm). c) Pixel size as a function of droplet volume. Adapted with permission from Ref. [5]. Copyright 2019, Wiley-VCH.

reported by Kang et al., who printed a photonic crystals based on a block copolymer (poly(styrene-block-quaternized 2-vinylpyridine)) to achieve a rewritable display (over 50 printing/erasing cycles).[100] The writing process involves a crosslinking agent (ammonium persulfate), while the erasing process is carried out with aqueous HBr. To ensure constant printing resolution, i.e. to avoid ink leakage on the edges of the pattern upon successive writing steps, the authors use grooved substrates (see Section 4.3).

Aside from quantum dots, other materials can be used for the development of optoelectronic devices, and in particular perovskite nanocrystals. Choi et al. synthesized cesium lead-halide perovskite colloidal nanocrystals that were formulated into inkjet-printable inks and coated as the color conversion layers of the quantum dot organic light-emitting diode hybrid displays. The device showed a photoluminescence quantum yield of ca. 96 % and a color reproduction range of 117 %.[101]

3.1.3. Inks for Energy-Harvesting Applications

Inkjet printing has already demonstrated its potential for fully printed organic solar cells.[102,103] However, the power conversion efficiency must be improved to match that obtained using conventional fabrication methods. Printing methods that increase the film homogeneity while decreasing the deposit thickness are still lacking. To balance the low inherent conversion efficiency of printed devices, large-area devices are required.

Thermoelectric materials (TEMs), i.e. materials capable of converting heat into electrical energy and vice versa, have attracted considerable attention in the last twenty years. Despite their relatively low energy conversion efficiency (5–10 %), TEMs are ideal candidates for the development of environmentally friendly energy sources, as heat is readily available energy from solar radiation and also the inevitable "side product" of almost any industrial activity. Inkjet printing is an interesting approach to pattern TEMs on a large-scale and flexible substrate, i.e. substrates that ensure efficient contact with the heat source. Despite these advantages, very few examples of printed TEMs have been published, most of them focusing on organic semiconductors (OSCs) or small molecules as active materials.[104–106] Thanks to the ability of inkjet printing to allow rapid fabrication of different layouts improved thermoelectric efficiency was recently obtained by coupling several thermoelectric cells on the same substrate (Seebeck coefficients in the range 22–27 $\mu V K^{-1}$ and power factors around 1 $\mu W m^{-1} K^{-2}$).[107,108]

Another growing application of inkjet printing for energy-harvesting applications concerns triboelectric generators,[109–111] which have recently taken advantage of the development of new printing methods for the deposition of the active piezoelectric material.[112,113]

The fields of application benefitting most from inkjet technology are identified in this section, and each convincing proofs of concept have been reported for each of them. Inkjet printing is undoubtedly a method of choice for the localized deposition of functional (nano)materials. However, all of these studies underline the necessary optimization of printing conditions to obtain an arrangement of active materials that is controlled in terms of spatial location, deposit shape (sharp edges), and homogeneity (thickness). Any improvement in this direction may have concrete consequences on the printed devices' figures of merit, as soon as very thin and uniform deposits are achieved.

3.2. Strategies toward Homogeneous Deposits

The capillary and convective processes occurring during ink evaporation fully establish the final distribution of (nano)-materials. Many studies continue to focus on a better understanding of the physical chemistry underlying the capillary and convective processes at work during the evaporation of inks. Recent reviews will give interested readers a more comprehensive and detailed view of this field.[114,115] In this section, we discuss the already known and updated strategies aiming to adapt the ink formulation in order to control the material distribution.

As mentioned in Section 2, the drying of a pinned sessile droplet (i.e. CCR evaporation mode) deposited on a substrate can lead to the formation of a large set of features, from uniform shapes to coffee rings. The coffee ring effect has long been seen as a disadvantage detrimental to the performance of the printed devices. Strategies have been developed to counteract and reduce the coffee ring effect: sliding the three-phase contact line,[116] reducing the outward capillary flow, inducing the inward Marangoni flow by the addition of a co-solvent with a low surface tension and a high boiling point,[1,117] adding additives such as polymers to increase the viscosity of the ink or surfactants[118] to limit the outward capillary flow, and controlling the substrate temperature.

3.2.1. Promoting the Inward Marangoni Flow

Du et al. have shown that by controlling the polarity and the viscosity of the ink it is possible to suppress the contact line receding and coffee ring effect during inkjet printing of small-molecule-based inks.[119] Solvents with polar groups, such as cyclohexanone, make it possible to pin the contact line and then suppress its receding. Addition of high-viscosity and high-boiling-point co-solvents such as cyclohexylbenzene and benzyl alcohol reduces the capillary flux and counteracts the coffee ring effect to form a homogeneous film. Kim et al. have printed Ag conductive electrodes onto polyimide substrates.[72] The addition to a mixture of solvents (ethanol, *n*-propanol, deionized water) of a high-boiling-point solvent (ethylene glycol) with lower surface tension suppressed the droplets' coffee ring formation and improved significantly the homogeneity of the deposit and, by consequence, the conductance of the printed electrode. The higher evaporation rate at the edge of the droplet and the differences in evaporation rates of the mixture of solvents composing the ink lead toa concentration gradient of the ethylene glycol component and, as a consequence, a

surface tension gradient within the sessile droplet. An inward additional Marangoni flow from the edge of the droplet (low surface tension) to the center of the droplet (high surface tension) leads to a uniform deposit of Ag nanoparticles.

The coffee ring effect can also be removed significantly by increasing the viscosity of the ink by the addition of surfactants[4,6] or polymeric matrices.[7,9,12,13] To overcome the higher evaporation rate of the solvent from the edge of the deposited droplet, the substrate can be heated to increase the drying rate of the solvent and attenuate or even suppress the coffee ring effect. Wang et al. have reported the uniform deposition of an aqueous ink based on pH-sensitive polymer-embedded palladium nanoparticles on an ITO glass substrate heated up to 50 °C.[120] Lee et al. have also optimized both the substrate temperature and the spacing of droplets to control the evaporation rate of the ink and counteract the coffee ring effect.[121] Ag gate and source/drain electrodes were printed on bare glass and poly(methyl methacrylate) (PMMA) coated glass for the fabrication of organic thin-film transistors (OTFTs). The authors showed that the width of the printed electrode exponentially increased when the temperature decreased and the accumulation of nanoparticles at the periphery of the printed lines decreased significantly.

3.2.2. Tuning the Colloid Distribution through Interactions between Ink Components

Talbot et al.[122] have reported the evaporation-driven sol–gel transition[123,124] of a suspension of laponite (a synthetic nanometric clay) to control the radial flow inside a sessile droplet. Upon evaporation, droplets of inks containing laponite and a polystyrene-sphere gel moved from the pinned contact line inward, reducing the radial motion of particles and then producing uniform depositsThe elasticity of the gel results from the "house of cards" structure formed by the assembly of the platelike laponite particles with their negatively charged faces and positively charged edges to form a network. By varying the laponite concentration, one can modulate the radial flow and control the final shape of the deposit from ring to pancake or dome morphology. To prevent aggregation of the polystyrene particles, colloidal silica was added to the ink formulation. A similar study with a water-soluble polymer (hydroxyethylcellulose) showed that laponite was more effective at suppressing ring stains. A rapid sol–gel transition in a binary solvent mixture (50 vol % ethanol/water) containing a low concentration of fresh hydrophobic fumed silica nanoparticles has also been demonstrated.[125] As ethanol evaporates preferentially from a picoliter droplet, hydrophobic interactions between the NPs are enhanced within the water-rich layer near the free surface, leading to the agglomeration of NPs and the formation of a 3D elastic network below the gas–liquid interface. Marangoni flow is then suppressed, thus finally leading to a uniform deposit.

Al-Milaji et al. employed a dual-droplet inkjet printing configuration to transpose the Langmuir–Blodgett (LB) technique to the picoliter droplets ejected from an inkjet printer.[126–128] Monolayers of closely packed nanoparticles were obtained by consecutive dual-droplet printing of a supporting droplet and a wetting droplet containing polystyrene (PS) nanoparticles. When the colloidal suspension spread over the surface of the supporting droplet, nanoparticles self-assembled at the interface between the wetting droplet and the supporting droplet. After evaporation of the solvent, a well-ordered deposition of nanoparticles was achieved (Figure 6).

The formulation of the inks plays a major role in the control of the formation of a homogeneous film: the surface tension of the wetting droplet should be lower than that of the supporting droplet to enable initial spreading. It has been demonstrated that the nature of the functional groups and the electrostatic interactions between nanoparticles affect the spreading of the wetting droplet and the morphology of the deposited film. The deposition of carboxyl-PS particles strongly depends on the pH of the supporting droplet and changes from coffee ring patterns at high pH to nearly uniform monolayers at low pH.[128] At pH >7, the zeta potential (absolute value) of the carboxyl-PS particles increases, leading to high particle–particle electrostatic repulsion. The self-assembly of the carboxyl-PS particles at the air–supporting droplet interface is then inhibited. The hydrophilic particles diffuse into the bulk of the supporting droplet and are subject to capillary flow, resulting in their accumulation at the edge of the droplet. In contrast, the pattern of the deposition of sulfate-PS particles is less impacted by the pH of the supporting droplet and a uniform monolayer is achieved regardless of the pH.

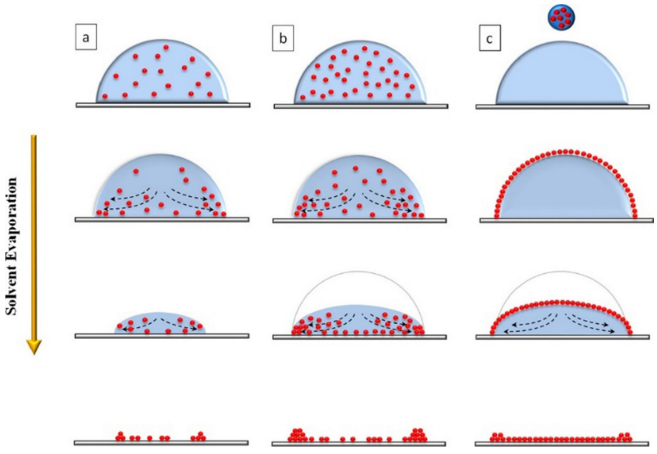

Figure 6. Schematics of conventional inkjet printing and dual-droplet inkjet printing of particle-laden droplets. a) Conventional inkjet printing of sessile droplets with low particle loading that depicts the depinning/pinning behavior of the contact line. b) Conventional inkjet printing of particle-laden droplets with high particle loading. The particles migrate and concentrate at the contact line by virtue of the evaporation-induced flow, causing the contact-line pinning. c) Dual-droplet printing process, where the contact lines remain pinned during solvent evaporation. The middle of the deposit is composed of a nearly closely packed monolayer of nanoparticles. Adapted with permission from Ref. [127].

3.3. Strategies toward Heterogeneous Deposits

Although uniform deposits have been mostly targeted so far, the formation of non-uniform deposits has nevertheless also been a goal in recent years. In 2000, Cuk et al. showed that drying liquid ribbons of solutions of copper hexanoate deposited by ink jet printing leads to solute segregation into multiple pairs of stripes.[129] This pioneering result showed that the coffee ring effect allows the formation of metallic lines much narrower than the initial ribbon diameter. In 2006, a second step was taken when the team of J. Moon studied the effects of the solvent composition on the homogeneity of inkjet-printed linear patterns composed of nanoparticles (silica[117] and silver[72]). Although their study aimed to minimize the coffee ring effect, incidentally they showed that nanoparticles could self-assemble at the edge of the pinned contact line to form a pair of continuous solid "twin lines" when the coffee ring effect occurs. In the case of silver nanoparticles, they showed the conductive character of these fine deposits. Starting in 2009, this effect has been used on purpose to print transparent conductive patterns, and arrays obtained by interconnecting metal rings or metal lines.[71,130–138] These conductive films are a potential alternative to tin-doped indium oxide (ITO) since the as-obtained arrays have better transparency and resistivity than conventional ITO transparent thin films.[130] Since 2009, this type of approach has been used for different combinations of colloidal inks and substrates: silver nanoparticles/poly(ethylene terephthalate) (PET),[136,137] silver nanoparticles/glass,[71] poly(dopamine) nanoparticle/PET,[132] carbon nanotubes/PET,[133] carbon nanotubes/p-type silicon,[134] graphene oxide/SiO_2,[135] titania particle/glass or PET,[138] and silica/Si wafer.[117]

Current development trends include the control of the line morphology and interline distance by adjusting the substrate weighting angle, the contact line depinning during drying.[139] The formation of twin lines is only one of many phenomena that have been identified over the last 20 years by macroscopic drop drying. Therefore, in the future, we expect a diversification of the heterogeneous patterns formed, in line with the recent work described by Bridonneau et al. (Figure 7).[139]

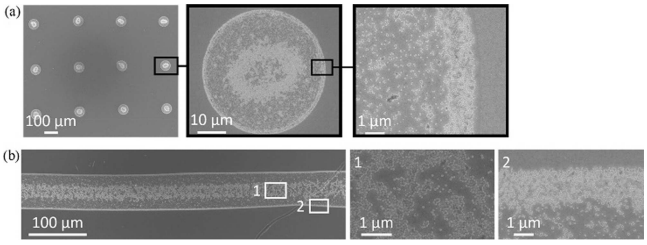

Figure 7. a) Typical SEM images of dry deposits from unfused droplets deposited by inkjet printing, with $\Delta x > D = 47$ µm, at different magnifications. b) Typical SEM images of dry deposits from fused droplets deposited by inkjet printing, with $\Delta x = 47$ µm $x < D$, at different magnifications. Adapted with permission from Ref. [139]. Copyright 2020, American Chemical Society.

In recent years, several authors have used magnetic or electric fields to tune the deposit features. For instance, Al-Milaji et al. reported an efficient suppression of the coffee-ring effect when the deposition of ferromagnetic Gd_5Si_4 particles was carried out under a magnetic field.[140] This finding could be of high importance for the design of nanostructured materials, as it could help tune the magnetic anisotropic properties. Following the same strategy, Jacot-Descombes et al.[141] and Song et al.[142] reported on the successful microstructure manipulation of Fe_3O_4 nanoparticles embedded in a polymer matrix through the application of a magnetic field. Depending on the magnetic field orientation, the nanoparticles formed dense continuous magnetic lines that could be oriented either in plane or out of plane. In a similar way, the application of an electric field can induce drastic changes of the deposited layers. As an example, Kamal et al. demonstrated the fabrication of electrically tunable bifocal liquid crystal (LC) microlenses using drop-on-demand inkjet printing.[143] In the presence of an applied voltage, the nematic LCs are deposited in a specific orientation, thus giving a larger refractive index along the detector. It was also shown that for a specific voltage range, two separate domains of the LC droplet could be formed, each showing a distinct refractive index profile. This efficient method to induce the assembly of nanoparticles upon ink drying is, however, restricted to a limited set of materials.

Finally, the "twin-line deposition method" allows high spatial resolution without the need for a special nozzle design or the application of an external electric field between the nozzle and the substrate. It has been shown experimentally that the width of a single line (w) can be minimized down to 2 µm by minimizing the drop size (D) based on the fact that $w \propto D$ for individual drops.[144] Qualitatively, this relation reflects the observation that the solute initially dispersed in the drop, which has a volume proportional to D^3, is finally deposited in the external ring, whose volume is proportional to Dw^2 so that $w \propto D$. Given the limited range of individual drop size (i.e. 20–80 µm), w can be further minimized by increasing the drop spacing to the limit of "stable" coalescence,[69] increasing the temperature to speed up evaporation,[134] and/or increasing the advancing contact angle.[145]

3.4. Concluding Remarks

The tailoring of capillary phenomena during ink drying is a relevant approach to achieve printed patterns that have nanoscale properties. Nevertheless, the deposits have high characteristic dimensions, i.e. several tens of micrometers, which are prohibitive in some situations. For these applications, it is necessary to improve the resolution, probably by developing alternatives such as those proposed in Section 3.2. However, new issues arise as soon as more than one functional ink must be printed.

Highly integrated devices require many elements, e.g. data processing and communication, energy generation, storage, and delivery and, for bioelectronics applications,

biological functions such as enzymes, nucleic acids sequences or even living systems (cell, microorganism, etc.).[25,146,147] Full inkjet fabrication processes necessitate the printing of several functions, i.e. several inks, on a given substrate with the same resolution. Assuming that the surface energy of the substrate remains the same throughout the printing process, and according to the great chemical diversity of materials that have to be printed (from hydrophilic bio-inks to organic solvent-based inks), the ink wetting properties must be tuned accordingly. However, nanoparticle- or biomolecule-based formulations cannot be changed while maintaining, at the same time, the integrity of the ink constituents, i.e. without avoiding flocculation (nanoparticles) or irreversible unfolding (biomolecules) of constituents. Hence, coplanar printing of different inks possessing different substrate affinities constitutes a current unaddressed issue in full inkjet device fabrication if one aims at obtaining well-defined, homogeneous layers.

From a more fundamental point of view, we can regret the absence of general (at least empirical) laws based on the printing conditions and the structure of the final printed pattern. This would be possible only if researchers describe more precisely the printing conditions, the parameters and materials of the systems used (solvent, solute, substrate), and the structure of the solid deposit (i.e. electronic microscopy, profilometry). This way, it would be easier to establish general laws that could be used as a guide for users.

4. Tailoring the Substrate Surface Energy and Topology

4.1. Substrates for Inkjet Printing

Trends in printed electronics are related to the integration (packaging, textiles, etc.) of several functions on the same device for applications in energy production/storage, (bio)-detection, and data display/communication. These applications require the printing of several inks with non-equivalent physicochemical properties and formulations with limited possibility of composition modification, given the constituents (nanoparticles, biomolecules, etc.). It is then necessary to develop inkjet printing-based functionalization approaches making it possible to tune the surface energy/topology of the substrate in order to adapt it to the ink to be printed. The use of printing methods is central because they allow localized modulation of the wettability properties of a substrate and thus coplanar printing of different inks with the same quality. The objective of this section is to review the methods used to control capillary processes during ink drying through prior modification of the substrate in terms of chemical composition (surface energy) and topology, focusing on the most often used substrates in inkjet printing (see Table 2).

4.2. Tuning the Substrate Surface Energy

Modulating the surface energy of the entire substrate to improve the resolution of printed patterns is well established.[155] The most common processes are treatments with plasma and UV–ozone which, in addition to removing organic contaminents from the surface, also introduce hydrophilic functions. Kwon et al., for example, succeeded in significantly removing: bulging instability of printed Ag lines by treating glass substrates with a C_4F_8 plasma containing a variable proportion of O_2.[156] The pure C_4F_8 plasma leads to the gas-phase deposition of hydrophobic fluoropolymers, while O_2 is degraded and -OH functions are introduced, thus modulating the surface energy of the substrate. In general, plasma treatment is mainly used for organic substrates such as PEN[157] and polyimide[158] based substrates. Poorly hydrophilic, these substrates require O_2 plasma or UV–ozone treatment to improve the printing resolution with water-based inks. However, the change in the surface energy following such treatment is reversible and the contact angle returns to its original starting value within a few hours.[159] This aspect considerably limits the use of this approach for the fine control of the wettability properties of a given substrate. In contrast, modulating the surface energy by chemical grafting approaches bypasses these issues. On the one hand, the use of a molecule containing a surface-anchoring function makes it possible to consider a stable modification of the substrate. On the other hand, the chemical modification of the substrate makes it possible to generate an apparent surface energy fixed by the chemical nature of the distal function of the grafted molecules.

Most of the current surface functionalization methodologies can be used to adapt the surface energy of a substrate to a given ink. Grafting thin organic films onto substrates such as borosilicate and Si oxide type materials (silanol chemistry), metal oxides (carboxylic acids), and also noble metals (alkylthiol chemistry) is well established.[160]? Several studies aimed at improving the printing process

Table 2: Physicochemical characteristics of some substrates often used in inkjet printing.

Substrate	Chemical composition	E_{Surf} [mN m^{-1}][148]	θ_{eq} [deg]
PET	Polyethylene terephthalate	44[148]	81[149]
PEN	Polyethylene 2,6-naphthalate	40[150]	66[150]
Kapton®	Polyimide	47[151]	70[152]
Silicon	Si	67[148]	21[153]
Glass	SiO_2	50–60[148]	57[154]
Borosilicate	SiO_2 B_2O_3	43[148]	63[148]

quality by grafting molecules to the surface using siloxanes.[28,161] Schlisske et al. studied in detail the influence of the self-assembly of different fluorinated and non-fluorinated siloxanes on the wettability properties of silver inks on common substrates (polymers, glass, and metal).[148] They were able to reduce the radius of a drop by 70% by modulating the surface energy through siloxane surface grafting. The formation of a bond between the substrate and the layer is effective on borosilicate substrates. On other substrates (metals, polymers), it is the crosslinking of the silane functions (polymerization) that allows the precipitation of (insoluble) material on the surface. The stability of this type of modification can be questioned in the case of the use of non-aqueous inks capable of resolubilizing the polysiloxane. Note that there are very few chemical functionalization processes for polymer substrates, which are particularly inert in terms of reactivity. Spin/spray and dip-coating type methods are the preferred approaches for modulating the wettability properties of PEN, PET, and polyimide-type materials.

The combination of chemical grafting methods and plasma or UV–ozone radiation can be used to develop methods for substrate microtexturing for inkjet printing applications (Figure 8). Lee et al.[165] and later Kim et al.[166] improved silver pattern resolution by exposing spin-coated fluorocarbon films to oxygen plasma. Depending on the conditions of plasma exposure (duration, power), the fluorocarbon layer is degraded and the hydrophilic/hydrophobic character of the substrate can be modulated. Nguyen et al. extended this approach using a PET substrate modified with a hydrophilic layer of 3-aminopropyl trimethoxysilane covered with a spin-coated hydrophobic layer made of a derivative of polytetrafluoroethylene.[162,163] The use of a Ni mask makes it possible to induce localized degradation of the hydrophobic layer and thus generate regular patterns with alternating hydrophobic zones ($\theta = 105°$)/hydrophilic zones ($\theta = 52°$). When printed on PEDOT:PSS, the ink follows the shape of the hydrophilic line and results in a line width equivalent to the width of the hydrophilic line (ca. 50 μm).

This work aims to reduce the maximum width of a printed line by constraining its spread through localized chemical modification of the substrate. Also based on chemical texturing, Sirrginhaus et al. proposed an innovative approach to generate sub-micrometric gaps by inkjet printing, thus breaking with the conventional resolution limit.[167] By making a micrometric stripeby photolithography and modifying it with a hydrophobic layer of perfluorodecyltrichlorosilane, the authors show that when a drop of PEDOT:PSS ink lands on this stripe, it splits in two and does not wet the surface modified by silane. The final deposit thus presents two continuous zones of PEDOT:PSS separated by a gap equivalent to the widthof the stripe, i.e. 250 nm. However original, this approach has been rarely used in inkjet printing to date, probably due to 1) the difficulty of positioning the drop in the center of the stripe,, and 2) the use of photolithography, which is not very compatible with the polymer substrates widely used in printed electronics.

The modulation of surface energy by chemical modification of the substrate or of a thin layer covering it makes it possible to control the size of the drop and thus to generate lines or gaps with a width less than the conventional limit of resolution of inkjet printing.

4.3. Template-Assisted Inkjet Printing

An alternative to chemical texturation consists in physically constraining the drop in furrows previously formed on the substrate by e.g. soft lithography or by hot stamping.[168] Keum et al. have described and modeled this principle of topography-directed inkjet printing (Figure 9).[169] This concept of template-assisted inkjet printing was used to produce QLEDs and LECs,[170,171] and extended to the production of nanostructured filtration materials and membranes.[172–174]

Other microstructure fabrication techniques have been used to control the wettability properties (orientation of capillary forces) and the dynamics of the contact line for improving printing resolution. Frisbie and co-authors have developed a remarkable method which they have called

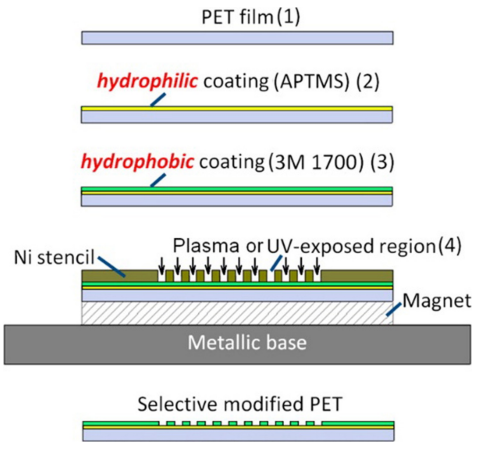

Figure 8. Process flow for patterning PET film with controlled wettability: 2) formation of a silica-like thin layer by dip-coating the PET film in a solution of 3-aminopropyl trimethoxysilane (APTMS) and acetone, 3) hydrophobic coating, 4) hydrophilic treatment to create to-be-printed features with the use of a Ni mask.[163]

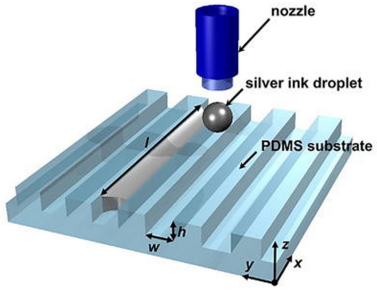

Figure 9. Schematic diagram showing the inkjet printing process on a structured PDMS substrate. Adapted from Ref. [169].

"self-aligned capillarity assisted lithography for electronics" (SCALE).[175–177] The method consists of using imprinted structures made up of reservoirs (radius of hundreds of μm) connected to channels (from a few micrometers to tens of micrometers in width and millimeters in length). The printing of an ink above the reservoir leads to the spreading of the ink into the channel connected to the reservoir over a distance depending on the amount of ink and the dimensions of the channel. Based on this SCALE principle, Frisbie's team produced many thin-film transistor-type devices and were able to achieve a resolution of a few μm in terms of the gap size between two printed metal contacts. (Figure 10).[177]

4.4. Full Inkjet Printing Process

Despite the advantages of an "all-inkjet" process, very few works have been published to date on the physical or chemical microstructuring of the substrate entirely by inkjet. Recently, Maisch et al.[178] elegantly leveraged the findings of fundamental studies investigating the ability of chemically textured[8] or dot-decorated substrates obtained by photolithography to modulate the dynamics of the contact line during droplet evaporation.[6,179,180] By inkjet printing dots of PEDOT:PSS on the substrate (i.e. ITO), they show a drastic improvement in the print quality of the subsequent layer made of an organic semiconductor. In the absence of the microstructure, the contact line retracts chaotically, resulting in a heterogeneous distribution not corresponding to the desired semiconductor pattern. The microstructures slow down the contact line recessing during ink evaporation, leading to a drastic increase in the resolution of the semiconductor pattern features.

Tseng et al.[181] proposed an "all-inkjet" approach inspired by the concept of "wetting-based self-alignment" initially developed by Sirringhaus et al. The interest here is the use of inkjet printing to generate terraces on which the printed ink drops divide, leading to deposition on either side (Figure 11). The loss of resolution linked to the use of inkjet printing compared to lithography to produce the terraces is here judiciously compensated by the modulation of the surface energy of the printed terraces. Indeed, authors printed poly(4-vinylphenol) onto the silver terraces. Improvement of the polymer thickness leads to a droplet that splits but does not roll to either side of the terrace. Finally, authors succeed in generating a gap of 0.47 μm by a full inkjet process. This approach has been rarely followed to date, certainly for the same reasons as those stated in the presentation of the seminal article by Sirringhaus (Section 4.2).

Another clever approach taking advantage of the coffee-ring effect was developed by Li et al. for the realization of an all-inkjet-made thin-film transistor (Figure 12).[182] The coffee-ring effect, which can be greatly modulated, leads to the accumulation of material in areas whose dimensions are much smaller than those of the initial drop.[114,183] In this article, the coffee ring formed by the evaporation of a hydrophobic polymer ink (CYTOP) is used as a template to define the dimensions of the transistor channel. The printing

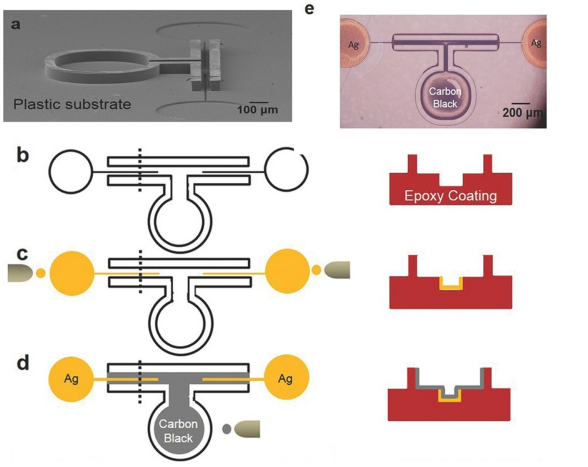

Figure 10. Fabrication of resistors using the SCALE process. a) SEM image displaying an imprinted device cavity on the surface of an epoxy/PET substrate for processing a resistor. b) Schematic of plan view of the device (left) and cross section along the dotted line (right). c) Metal electrodes are processed by inkjet printing an Ag ink into the yellow reservoirs (left). The ink is wicked into the channels by capillarity; a thin Ag film is left behind on the channel walls upon annealing (right). d) A carbon black ink is dispensed into the gray reservoir which wicks into the attached channel connecting the two metal electrodes in the process. e) Optical image of a completed device, adapted from Ref. [177].

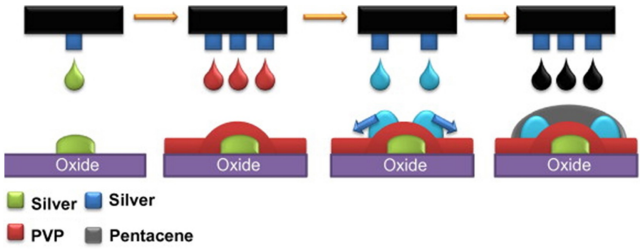

Figure 11. Inkjet transistor process with self-aligned Source/Drain electrodes. a) Inkjet transistor process, consisting of four layers of printing. Adapted from Ref. [181].

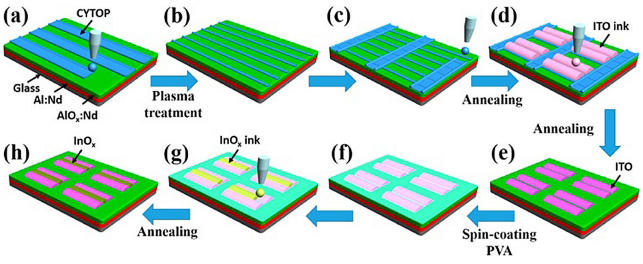

Figure 12. a) Printing a CYTOP line pattern. b) CYTOP coffee stripes. c) Printing CYTOP perpendicular to and onto predefined coffee stripes. d) Printing ITO ink onto the array of rectangular CYTOP framework. e) ITO electrode pairs. f) Modification of substrate with an ultrathin PVA layer. g) Printing InOx ink onto channel areas. h) Array of InOx TFTs, adapted from Ref. [182].

of an ITO ink shows that the ejected drop divides on both sides of each edge of the coffee ring, thus creating two conductive contacts (source and drain) separated by a distance equivalent to the widthof the edge, i.e. 2 μm. The successive printing of a semiconductor, an insulator, and a final conductive layer (gate) complete the transistor fabrication process. Electrical contacts with these dimensions make it possible to enhance the transistor output characteristics thanks to a marked increase of the channel length (length of an ITO line) to width (border thickness) ratio. This approach opens the way to the fabrication of transistor arrays over large substrates, including flexible and transparent ones.

4.5. Guidelines for Substrate Tailoring: Concluding Remarks

The analysis of the examples taken from the literature and reported in this section demonstrates that the nominal resolution limit of inkjet printing, around 50 μm, can potentially be improved by several orders of magnitude by tuning the substrate properties. A few guidelines may be formulated/given based on the examples and the theoretical foundations described in Section 2. For instance, the most important parameter fixing solid matter distribution at the substrate surface after solvent evaporation is the difference between the surface energy of the ink and the substrate itself. This difference may be increased by the introduction of microstructures (Cassie and Baxter model) and used, for instance, to contain the liquid within anisotropic spaces (lithography-made microstructures, template-assisted inkjet printing, drop splitting). Considering a CCA evaporation mechanism, the printed pattern will have a minimum dimension corresponding to the radius of the contact surface between ink and substrate. This dimension can be reduced by confining the ink within a preformed mold. Under these conditions, it is possible to obtain micrometer-sized patterns. Only approaches based on the "drop splitting" phenomenon[167] allow the fabrication of nanometer-sized structures, in the presence of microgaps of roughly a hundred nm. These approaches have been employed in important applications, but they rely on the utilization of photolithography for substrate prepatterning, which considerably reduces the advantages typically connected to inkjet printing (low fabrication costs, large-area substrates). The major interest is therefore in methodologies relying on inkjet printing to introduce sub-micrometer structures on large surfaces.

The most efficient approach is to induce a heterogeneous organization of the solid content of (nano)colloid-based inks in order to obtain large-area patterns showing sub-micrometer resolution. In order to obtain nanometer-sized structuring starting from ink droplets measuring a few micrometers, the approach most commonly used is amplifying the coffee ring effect. To this end, the following main factors can be exploited (see Sections 2.3 and 3.2 for more detailed descriptions):

- *Drying mechanism*: The CCR mode is necessary to induce an inhomogeneous distribution of the colloidal constituents of the ink. If one aims at obtaining a heterogeneous deposition, one needs to increase the intensity of all phenomena able to block the contact line, such as using a rough substrate and maximizing the contact angle (ideally, higher than 90°). Other phenomena that can be exploited are the convective flows. These flows can be increased by carefully tuning the ink composition, i.e. by favoring the Marangoni flow (utilizing a low-boiling-point co-solvent, reducing the surface tension by adding surfactants, reducing viscosity).
- *Particle concentration*: The structure of heterogeneous solid deposits can be controlled by the initial concentration of particles in the deposited drops. For single drops containing a stable suspension of particles, at low concentrations, the particles preferentially deposit at the center of the initial drop footprint, forming dot-like patterns, while higher concentrations result in particle deposition at the periphery, forming a thick ring pattern, and finally deposition over the entire surface at high concentrations. The width of the outer ring, which is present throughout the concentration range, increases as a power law with increasing particle concentration.[144] Interestingly, it has been shown that by depositing individual drops of nanoparticle dispersion on a surface with a drop spacing that allows their coalescence, it is possible to form stable liquid streams that become solid continuous "lines" after evaporation of the solvent and self-assembly of the particles at the pinned contact line.[71] By means of this droplet fusion process, it is possible to transpose the variety of deposits obtained by drying individual drops into lines. The number of lines and the distance between the lines can be controlled by varying the volume of the initial drops and the concentration of the particles. Moreover, as in the case of isolated drops, there is a power law dependence of the thickness of the outer lines (i.e. a few microns) with the particle concentration.[139]

These parameters are not the only ones that can be used to modify the solid content distribution. It is indeed the combined set of both ink and substrate characteristics, taken as a whole, that determines how matter distributes during solvent evaporation. Publications on this topic unfortunately contain limited information on the experimental conditions to allow precise statements in the form of general rules. However, it is also likely that even if all experimental details were available, the formulation of general laws would be extremely difficult because of the very large number of parameters necessary to describe accurately the system dynamics (combination of several out-of-equilibrium processes, open systems characterized by heat and matter transfer). In this regard, the approaches based on machine learning would be probably highly relevant to correlate the morphology of nanostructures to the experimental conditions.

5. Outlook: What's Next?

5.1. From Micrometer- to Nanometer-Scale Organization of Constituents in Key Applications

Sections 2 to 4 presented the main methodologies to improve the spatial resolution of printed patterns. These methodologies make it possible to localize, with variable resolution, the deposition of inks and therefore to organize the functional constituents on a substrate, in the same plane (coplanar deposition) or by stacking (multilayered deposition). Inkjet printing is not particularly suitable for the fabrication of multilayered structures for the following main reasons: 1) A problem common to other liquid-phase deposition techniques is the need to adapt the composition of the inks to avoid the dissolution of the $(n-1)$th layer during the printing of the nth layer (extremely delicate with regard to the other constraints, in particular those related to the stability of nanoparticle-based inks); and 2) the thickness of the printed layers is generally greater than 100 nm. Theoretically, it is possible to reduce the concentration of the ink by several orders of magnitude to obtain patterns with a thickness down to a few nm, but several capillary and convective processes may occur and prevent the formation of homogeneous monolayers. The classic configuration of many emerging devices, in particular OLEDs, QLEDs, and OPVs, requires several stacks of a few nm each, which is not reasonable to obtain by inkjet printing and which requires the development of alternative geometries, in particular coplanar architectures.

The interest in inkjet printing for the fabrication of coplanar devices is reinforced by the possibility of functionalizing flexible, fragile, biosourced substrates, with virtually no limitations on the maximum surface that can be used for the fabrication of the devices. All applications based on exchange processes between the external environment and a functionalized surface (heat, absorption/emission of photons) can benefit from the increase in device size, e.g. increase in the contact surface with a heat source for thermoelectric devices, increase in the quantity of photons absorbed in the case of photovoltaic cells. Printing is an ideal solution for the deposition of the same material over large surfaces as well as for the repeated fabrication of devices (serialization of energy production cells, pixels). Furthermore, all applications based on the analysis or processing of liquid samples under flow conditions would benefit from innovations in manufacturing processes. Current microfluidics makes it possible to apply various electric fields to all the constituents located in a cross-section of the channel to trigger electrochemical or transport processes. The application of hydrostatic pressure in the channel allows circulation through an entire sample. This property is used for electrosynthesis under flux as well as for sample analysis (separation by electrophoresis, dielectrophoresis, etc.). These applications require maintaining a micrometric channel height to ensure that all the content flowing through the channel is addressed. Consequently, the analysis flow rates remain low (a few $\mu L\,min^{-1}$). Inkjet printing makes it possible to design electrode patterns on surfaces of the order of a cm^2.[184] The combination of these large-sized printed electrodes with simple microfluidics allowing a channel height of a few μm to be maintained directly leads to an increase in analysis throughput by several orders of magnitude. Nevertheless, even if the overall dimensions of the device can be increased on request, the control of the layout of the printed materials must be effective on scales determined by the property concerned. For most of these properties, the challenge in coplanar architecture is to print patterns showing characteristic dimensions below the micrometer scale.

Indeed, in coplanar configuration, almost all optoelectronic devices (transistors, diodes, photovoltaic or thermoelectric cells, etc.) have performances that depend on a form factor W/L with L a characteristic distance that must be traveled by charge carriers inside a material, for example to or from a current collector or channel length in a field-effect transistor, and W the length of the junction between two materials, e.g. p-n legs length in thermoelectric and p-n junction length in PV devices. W can be usually custom extended, but L depends directly on the lateral resolution of the printed patterns. An identical comparison can be made for analytical devices, in particular devices for separation by dielectrophoresis, the performance of which depends directly on the ability to generate significant electric field gradients. Realizing patterns of electrodes resolved at the scale of a hundred nanometers (micro-nanogaps) on large surfaces would make it possible to apply intense gradients and thus to separate under flow all the constituents of a sample, including nanometric objects (nanoplastics, viruses).

For inkjet printing to meet the demand in terms of functionalization of large surfaces, significant progress is still necessary to overcome the limit of micrometric resolution. It is necessary to aim for methods making it possible to achieve spatial resolution of the order of 100 nm, a dimension that makes sense for the majority of the applications considered. Improving the resolution of printed patterns by several orders of magnitude can only be achieved through alternative methodologies to the use of lithography steps (structuring of substrates) or the use of specific printing equipment that increase the manufacturing speed and present a prohibitive cost, respectively, despite improving resolution. It is then necessary to develop new printing paradigms that allow nanometric-scale resolution and are compatible with economically viable large-surface functionalization processes. In the organization of matter at the nanometer scale, alternatives should take advantage of benefits from capillary and convective phenomena as well as from self-assembly processes between the ink constituents and the substrate or in-between ink constituents. For such objectives, dedicated research generating new inks or new surface functionalization processes should be conducted by chemists. In this section we propose directions that could make it possible 1) to remove all or some of the obstacles limiting the resolution as well as 2) to illustrate the capacity of chemistry to devise innovative solutions.

5.2. Improving Equipment and New Paradigm for Droplet Formation

The limitation of DOD inkjet printing technologies is the size of the droplet, which limited mostly by the size of the nozzles. To address this issue, acoustic inkjet printing technology was developed.[185] It is a nozzle-less technique where droplets are generated by focusing a high-frequency acoustic wave (5–300 MHz) onto the surface of the liquid ink, which creates extremely small droplets 5 to 300 pm in diameter. However, the ability to jet droplets of constant size has to be improved and, as far as we know, this has not found industrial application yet. Another important issue is represented by the possibility of depositing on the same area different types of inks within a very short period, since the activation of many chemical reactions of interest requires the subsequent and rapid mixing of reagents. Even though most industrial printers (and also some printer models available for laboratory-scale production such as the Dimatix DMP3000 series and Ceradrop F-series) are today equipped with a printhead capable of holding several cartridges containing different inks, only one cartridge can be utilized at a time and the deposition of the nth ink pattern must wait until the preceeding $(n-1)$ layers have been completely printed and (possibly) cured.[186,187] Currently, the simultaneous printing of different inks at the same spot can be achieved only through homemade, multi-nozzle systems.

5.3. Reactive Inkjet Printing: A Step toward On-Site Generation of the Target Function

In many situations related to the printing of nanostructures, the stability of the suspensions is limited and any variation in formulation is likely to cause irreversible denaturation of the constituents (aggregation, reaction in the cartridge, etc.). Increasing the mass fraction of nano-objects in an ink is not easy and yet necessary in certain situations such as printing (semi)conductive inks. A recent alternative approach and to date probably too little considered is to synthesize the supramolecular objects or structures directly on the substrate by sequentially printing the reagents. The reactive inkjet process (RIP) is an emerging trend that pushes further the possibilities of the inkjet process by using reactive inks in which chemical reactions take place. This process be based on either a single-ink mixture hosting a chemical reaction, or two inks reacting with each other, leading to results that could hardly be obtained by other methods.

The reactive inkjet process was applied to the in situ synthesis of gold nanoparticles, as demonstrated in 2014 by Abulikemu et al.[188] The authors showed that AuNPs of very acceptable size and polydispersity (8 ± 2 nm) could be obtained by the deposition of first a mixture of the reducing agent and capping ligand (in this case oleylamine), then the gold precursor ($HAuCl_4{\cdot}3H_2O$), followed by a post-printing heat treatment at 120 °C. Following this trend, Ahn et al. synthesized polymer thin films of PVK (poly(9-vinylcarbazole)) with a control of its molecular weight, for OLED applications.[189] By controlling the monomer reaction via the concentration of radical polymerization initiator, they were able to select the polymer by molecular weight, which resulted in modifications of the electrical properties. This method is particularly easy to control and not expensive. In 2019, Teo et al. reported on the use of the micro-reactive inkjet printing (MRIJP) technique to deposit polyaniline (PANI)[190] and a conductive PEDOT/ionic liquid hydrogel (Figure 13).[191] The process developed by the authors requires only one printing step that involves the in-air coalescence of two reactive inks. This approach has several advantages as it obviates adjusting the deposition accuracy between two reactive layers and dealing with evaporation rate issues.

Based on this brief review of the current surface reaction processes already accessed by inkjet printing and considering the wide range of surface functionalization methodologies not yet addressed, there is still an extensive field of investigation open to research.

5.4. Current Surface Functionalization Approaches: What Should Be Transferred to Inkjet?

One of the most widely used approaches in the chemical functionalization of surfaces is atom transfer radical polymerization (ATRP), which is used to modify the substrate surface by grafting polymer brushes (thickness from few to hundreds of nm) characterized by extremely low size dispersion. A huge set of monomers can be polymerized through ATRP, allowing the modulation of the substrate surface energy to a large extent. ATRP has already been used in combination with inkjet printing (Figure 14).[192] The prior modification of an SiO_2 substrate by ATRP of polystyrene brushes modulates the evaporation dynamics of a TIPS-pentacene ink, allowing the production of semiconductor crystals. By printing the TIPS-pentacene between two electrodes, the authors show a drastic improvement in the mobility of charge carriers compared to bare SiO_2 substrate. Current ATRP catalysts require the absence of

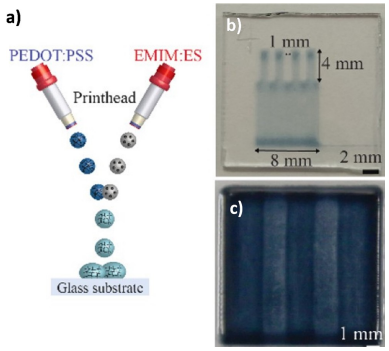

Figure 13. a) Proposed printing techniques allowing two different reactive materials to react in mid-air and form subsequently synthesized materials on substrates. b, c) Examples of patterns composed of conductive PEDOT:PSS/ionic liquid hydrogel. Adapted from Ref. [191].

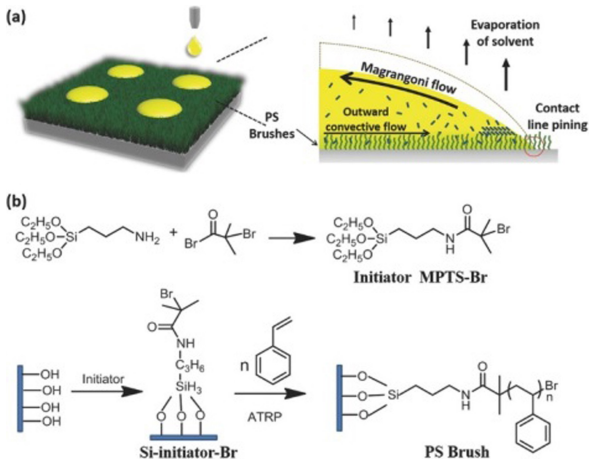

Figure 14. a) Schematic illustration of droplets inkjet-printed on PS brush-modified surfaces (left) and the possible mechanism through which the PS brushes impact the evaporation process (right). b) Synthetic route for PS brush attachment via the SI-ATRP method Ref. [192].

O_2, precluding interest for the application of inkjet printing. However, recent advances in ATRP catalyst design and synthesis that tolerate oxygen content unlock this main barrier and open new possibilities. Inkjet printing could now be used to implement several functionalities on a given substrate according to the same chemistry.

Other radical polymerization reactions can be considered for locally texturing a substrate by inkjet printing. Substrates showing reactivity toward organosilanes (borosilicate, SiO_2, etc.) or alkylthiols (noble metals) are good candidates for grafting by radical polymerization according to the commercial availability of polymer initiators functionalized by such chemical groups. However, there are very few methods compatible with ambient conditions to functionalize the most common substrates used in inkjet printing, i.e. plastic substrates. Indeed, selected for their chemical stability, plastic substrates have seen little innovation in their modification. Thus, one of the main substrates used in inkjet printing, PEN, cannot be chemically modified under mild conditions. On the other hand, there are several methodologies concerning PET and Kapton.

Modulation of the surface energy of PET by solution processes has the major advantage of being compatible with inkjet processes. Controlled radical polymerization processes (grafting-from, grafting-to) have proven their effectiveness in terms of modulating the hydrophobic character of PET surfaces[193,194] but have the main drawback of requiring a total absence of oxygen. Other processes such as the use of highly alkaline solutions allowing the production of surface COOH functions[195] or the thermally activated nucleophilic attack of primary amines on the carbonyl of PET[196] overcome this drawback but suffer from slow kinetics (several hours). On the other hand, diazonium chemistry represents a fast and extremely versatile class of reactions.[197] The C-aryl diazonium bond can be cleaved homolytically to give rise to a radical capable of reacting with a large number of organic functions, including those found onto PET.[198] This type of reaction can be implemented under mild conditions and therefore transferred to printing processes. Even though diazonium chemistry is a reference method for the modification of any type of surface, only Berthelot et al. have published a formulation based on diazonium salts. Under irradiation, a photosensitizer switches on the diazonium reduction and the formation of the corresponding aryl radical, which in turn initiates the polymerization of methacrylic acid (Figure 15).[199] Considering the variety of X-substituted acrylate-type monomers, the ability to modify the surface energy locally by inkjet printing seems strong.

Owing to its thermal stability, Kapton is a substrate widely used in inkjet printing. Few reports are related to polyimide based-substrate modification because of its chemical inertia, avoiding functionalization in mild conditions. Grandoni et al. showed that the exposure of Kapton to CF_4–O_2 microwave plasma allows an opening of the imide ring and the grafting of fluorinated substituents (increase of the contact angle).[151] A decrease in the contact angle can be induced when Kapton is irradiated by a UV source under an ambient atmosphere (oxidation of surface functions). Vural et al. have developed a versatile surface functionalization approach which consists of chloromethylating Kapton and then introducing an azide function.[200] The Kapton thus activated can be modified on demand by click chemistry reactions. The chloromethylation conditions require the use of aggressive solvents (chloroform) and reducing agent ($SnCl_4$) and the azide insertion step is slow,(24 h), all constraints that are hardly compatible with functionalization by inkjet printing. In an interesting and recent alternative, Kapton copolymers were developed containing a few imide units substituted by reactive functions. Liu et al. recently presented a Kapton containing carboxylic acid functions that allow the deployment of extremely rich and robust surface chemistry.[201]

The works reported above indicate that it is possible to use well-known surface functionalization methods in the inkjet printing context. The main issue probably lies in the

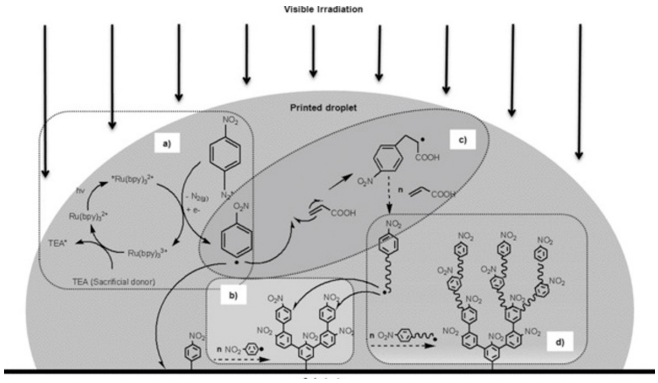

Figure 15. Proposed mechanism for in situ surface grafting a) Photo-assisted reduction of the aryldiazonium compound. b) Grafting of the resulting aryl radicals onto the surface and growth of the polynitrophenylene multilayer. c) Initiation of acrylic acid polymerization by the aryl radicals. d) Grafting of polyacrylic acid oligoradicals on the primer layer. Adapted from Ref. [199].

first step, i.e. the activation of the substrate through the grafting of a first molecular entity. Once this step has been completed, it can then be envisaged to extend the principle of grafting to molecules bearing chemical functions capable of serving as an anchoring point for further surface chemistry methods. Beyond the localized introduction of functions, the controlled grafting of molecules on a substrate by printing also finds a direct application in the modification of the substrate prior to the printing of a functional ink. Indeed, we underline in Section 3 that an elegant approach to improve printing resolution of a functional material is to decorate the substrate through chemical (distribution of surface energy) or physical (topology) microstructuration. Surface grafting methods are versatile and may be considered to locally tune the substrate surface energy and by consequence to control the wetting behavior of the ink printed in the following steps.

5.5. Stimuli-Responsive Colloids for Controlling Capillary Processes

Continuous advances in the understanding of capillary and convective processes, recently reinforced by modeling approaches, show that the dynamics of the contact line control the final pattern obtained after the evaporation of a colloidal ink. There is therefore a strong interest in developing colloids capable of switching their physicochemical characteristics and/or their reactivity toward the substrate under the impulse of a stimulus to make it possible to block or release the contact line on demand. For example, colloid property switching could be sufficient to alter substrate/colloid or colloid/colloid interactions to a large extent, leading to the sudden appearance (or dispersion) of aggregates and pinning (or release) of the contact line. For this approach to be efficient, the switching rate of colloid properties must be faster than that of a classical contact line dynamics. Developing this type of approach would lead to real innovation in the field of template-assisted inkjet printing by allowing localized chemical (surface energy of colloids) and topological (coffee-ring or terraced structure) texturing. The difficulty lies possibly in the development of nanoparticles whose corona can switch its physicochemical characteristics and/or its reactivity toward a substrate at a very high rate. This theme is currently at the center of many research efforts but for applications mainly in nanomedicine.[202] Among the most studied materials, polymers of the poly(*N*-isopropylacrylamide) (PNIPAM) type and their variations as copolymers (i.e. PNIPAAm-*co*-polyacrylamide, PNIPAAm-*co*-poly(methylmethacrylate), etc.) have many advantages in terms of molecular switching. Under the influence of an increase in temperature (critical temperature around 30–40 °C), macromolecules change from a compact hydrophobic state to a swollen hydrophilic state. These materials, produced by controlled radical polymerization, can be obtained in the form of an extremely thin brush (a few tens of nm) on different types of surfaces and even those of nanoparticles. To date, this type of material mainly shows switching rates of the order of a second[203,204] but more recently, an in situ kinetic measurement of polymer brushes shows that this time scale can be improved by decreasing the film thickness (i.e. thickness of 80 nm, $t_{switch} = 0.48$ s) as well as the polymer chain density.[205] Ding et al. studied individually PNiPAM-functionalized Au nanoparticles (polymer thickness 70 nm) and showed that the switching rate is instantaneous (i.e. < 1 ms).[206]

Nanoparticles functionalized by such photoswitchable macromolecules have a major advantage since they may switch their properties several times during the evaporation process. New classes of hydrogels consisting of polymer chains functionalized by photosensitive molecules capable of generating reversible crosslinking under irradiation are under development.[207,208] Although mostly used in the form of bulk materials, the current examples exhibit switching times (several min) that are not compatible with those of inkjet printing evaporation processes. Particular attention should be probably paid to the development of colloids functionalized by thin layers of stimulable macromolecules which, under irradiation, cause ligation of the colloids, and therefore a change in their apparent size.

Another way to perform instantaneous modifications of the substrate's surface chemical composition is to use monomer-based inks leading to polymer deposition upon irradiation. This methodology has advantages over classical 3D printing, first and foremost the ability to generate submicrometric thick layers. Based on recent advances both in terms of the type of ink now suitable for 3D printing under mild conditions (large choice of materials, e.g. photopolymerizable biomaterials, hydrogels)[209] and in the know-how of surface functionalization by photopolymerization,[210] the possibility of formulating inks containing both photoinitiators and monomers is real and would constitute another approach to surface microstructuring by inkjet printing. In inkjet printing, localization is dictated by the nozzle and the use of a much less complex light source becomes possible. The absence of the need for focusing the light source makes it possible to consider all wavelengths and therefore an extremely wide range of photochemical reactions. The real constraint to the deployment of this type of strategy lies in the development of a radical polymerization mechanism tolerant to the presence of dioxygen.[211] However, this field is constantly evolving and is a source of inspiration for the increase in substrate microstructuring methodologies based on inkjet printing.

5.6. Forthcoming Issues Related to Sustainable Substrates

Since it may be possible to print an infinite variety of materials, including biocompatible compounds, the use of inkjet for the functionalization of living tissue is expected to experience intense development in the years to come. The main obstacle to be overcome, given the specificity of these substrates (temperature variation, significant humidity, elasticity, etc.) is the design of a functionalization methodology guaranteeing high print resolution and stable adhesion of the patterns. One approach could be the development of a versatile material that makes the substrate compatible with

the characteristics of the printing ink, a material that contains a function compatible with the substrate and another that modulates the surface energy. As such, the use of polymers seems to be a priority.

Current inkjet printing substrates are mainly of petrochemical origin. Flexible, transparent, and low-cost, they have certain advantages but will eventually have to be replaced by bio-sourced or biodegradable substrates. As such, cellulose-based substrates meet most of these criteria (except transparency). However, they have the particularity of being fibrous in their unprocessed version. Most inks, especially hydrophilic ones, exhibit extreme wettability characteristics and swell the cellulose fiber matrix very quickly (Figure 16). Macroscopically, the ink droplets diffuse in depth as well as laterally from their impact position, a process resulting in a crippling loss of resolution. To overcome this problem, the solutions adopted for a long time have consisted in modifying the entire substrate with several thick layers of polymers (several micrometers). This treatment strongly compromises the biodegradability of the cellulosic substrate. To circumvent this problem and ensure biodegradability, it is possible to deposit a monomolecular layer by various methods now well mastered,[212] at the center of which is the condensation of silane functions.[213] However, these cellulose modification processes are carried out by immersion, producing a homogeneous substrate in terms of surface energy. The current need to print, in a coplanar manner, various functional inks, especially with variable wettability characteristics, requires a localized modification of spatial resolution. Impressive advances have been made in recent years in the development of disposable paper detection strips.[214] However, their spatial resolutions hardly reach 0.5 mm for the reasons mentioned above. It is therefore necessary to develop methods for adapting the wettability characteristics of cellulose fibers by first printing an ink that alters the surface chemistry of the fibers, i.e. modulating their surface energy. Again, it is worth exploring the solutions implemented in other fields of application to first perform a surface energy mapping and then print the desired inks in a controlled manner. The strong demand for a device manufacturing process on cellulosic substrates should lead to further advances in this field.[215]

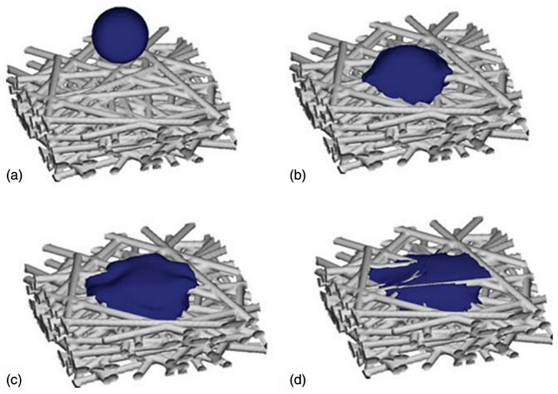

Figure 16. Illustration of droplet absorption into a porous medium such as paper: a) droplet arrives on the substrate at high speed, b) spreads upon impact, c) spreads by capillarity, d) and is absorbed within the medium. Reproduced from Ref. [216].

The third limitation, which may be the most restrictive, is due to the interactions between the ink and the substrate. For instance, the surface energy of the substrate with regard to that of the ink is also a major limiting parameter. Also, droplets that are expelled at a speed between 3 and 15 $m\,s^{-1}$ spread upon impact, coalesce, and/or are absorbed. These processes contribute to limiting the lateral resolution because the final dot is necessarily (under these conditions) larger than the diameter of the droplet.

One of the growing trends is to implement functions directly on living tissues such as skin (tattoo printing[217,218]) as well as plant tissues. There is a strong demand for new 1) sensitive or 2) active devices. The ability to implement detection functions on living tissues would make it possible, on the one hand, to control the environment in contact with the tissue (humidity, temperature, pollutants, etc.) and on the other hand, to perform a diagnostic (biosensor, e.g. control of glycemia, markers of inflammation, infection, etc.).

In addition, printing active components on these tissues capable of being activated on demand would lead to a new generation of devices for recreational applications (displays, release of volatile compounds, e.g. perfumes), prosthetics,[219] and agri-food with the possibility of functionalizing plant tissues for the control of the plant's adaptive response to stress.[220] To date, apart from an example of direct printing on plant tissues[221] (humidity sensor printed on a tree leaf) the strategy adopted consists of printing on conformable substrates, themselves positioned on the surface to be analyzed.[222]

6. Conclusion

Inkjet printing methods are of growing interest in many scientific areas, benefitting from advances made in related fields (technological innovations, nanochemistry, supramolecular chemistry, etc.) and feeding dynamic fields of applications such as optoelectronics, energy harvesting, and biomedical devices. This is mainly because inkjet printing handles dilute inks and deposits them in very small liquid volumes, at precise locations while minimizing surface contamination and ink waste. Inkjet printing is consequently the most suitable technique among additive fabrication methods for printing with high added-value inks.

Today's inkjet printing throughput still does not compete with that of contact printing techniques (e.g. gravure, flexography). It is therefore unlikely that full inkjet printing manufacturing processes will emerge. Inkjet printing, on the other hand, is relevant for intervening in a phase requiring the localized and controlled introduction of one or more functions, all of the other stages (metal contacts, encapsulation, etc.) being ensured by other printing methods. All the innovations leading to this or these inkjet printing step(s) improvement(s), in particular in terms of spatial resolution

of the printed patterns, will find direct application in a very large number of technologies.

The performance of printing equipment and its diversity are constantly improving and will continue to lead to technological advances, but it is the chemistry that will produce the expected innovations needed to fulfill the increasing demand in functional printed devices. Indeed, the synthesis and formulation of functional inks, the development of strategies for adapting the physical and chemical characteristics of surfaces, as well as the design of new printing paradigms (switchable, reactive inks) are development areas for which chemists will be the driving force.

Acknowledgements

J.L. thanks the ED 388 for his PhD grant.

Conflict of Interest

The authors declare no conflict of interest.

Keywords: Inkjet Printing · Printed Electronics · Reactive Inks · Sessile Droplets · Surface Functionalisation

[1] Y. Z. N. Htwe, W. S. Chow, G. Suriati, A. A. Thant, M. Mariatti, *Synth. Met.* **2019**, *256*, 116120.
[2] M. Orrill, D. Abele, M. Wagner, S. LeBlanc, *J. Colloid Interface Sci.* **2020**, *566*, 454–462.
[3] A. R. Hopkins, D. C. Straw, K. C. Spurrell, *Thin Solid Films* **2011**, *520*, 1541–1545.
[4] H. Radman, M. Maghrebi, M. Baniadam, *Diamond Relat. Mater.* **2019**, *100*, 107550.
[5] P. Yang, L. Zhang, D. J. Kang, R. Strahl, T. Kraus, *Adv. Opt. Mater.* **2020**, *8*, 1901429.
[6] N. Lin, Y. Ye, Q. Guo, J. Yu, T. Guo, *J. Inf. Disp.* **2020**, *21*, 113–121.
[7] B. Begines, A. Alcudia, R. Aguilera-Velazquez, G. Martinez, Y. He, R. Wildman, M.-J. Sayagues, A. Jimenez-Ruiz, R. Prado-Gotor, *Sci. Rep.* **2019**, *9*, 16097.
[8] M. Shariq, S. Chattopadhyaya, R. Rudolf, A. Rai Dixit, *Mater. Lett.* **2020**, *264*, 127332.
[9] Y. Hao, J. Gao, Z. Xu, J. Luo, X. Liu, *New J. Chem.* **2019**, *43*, 2797–2803.
[10] I. Fernandes, A. Aroche, A. Schuck, P. Lamberty, C. Peter, W. Hasenkamp, T. Rocha, *Sci. Rep.* **2020**, *10*, 8878.
[11] A. Kosmala, R. Wright, Q. Zhang, P. Kirby, *Mater. Chem. Phys.* **2011**, *129*, 1075–1080.
[12] A. Mavuri, A. G. Mayes, M. S. Alexander, *Materials* **2019**, *12*, 2277.
[13] A. Chiolerio, M. Cotto, P. Pandolfi, P. Martino, V. Camarchia, M. Pirola, G. Ghione, *Microelectron. Eng.* **2012**, *97*, 8–15.
[14] J. Kastner, T. Faury, H. M. Außerhuber, T. Obermüller, H. Leichtfried, M. J. Haslinger, E. Liftinger, J. Innerlohinger, I. Gnatiuk, D. Holzinger, T. Lederer, *Microelectron. Eng.* **2017**, *176*, 84–88.
[15] I. Pereiro, J. Cors, S. Pané, B. Nelson, G. Kaigala, *Chem. Soc. Rev.* **2019**, *48*, 1236–1254.
[16] S. Azizi Machekposhti, S. Mohaved, R. J. Narayan, *Expert Opin. Drug Discovery* **2019**, *14*, 101–113.
[17] L. Nayak, S. Mohanty, S. K. Nayak, A. Ramadoss, *J. Mater. Chem. C* **2019**, *7*, 8771–8795.
[18] M. Gao, L. Li, Y. Song, *J. Mater. Chem. C* **2017**, *5*, 2971–2993.
[19] G. Mattana, A. Loi, M. Woytasik, M. Barbaro, V. Noël, B. Piro, *Adv. Mater. Technol.* **2017**, *2*, 1700063.
[20] Q. Huang, Y. Zhu, *Adv. Mater. Technol.* **2019**, *4*, 1800546.
[21] Z. Zhan, J. An, Y. Wei, *Nanoscale* **2017**, *9*, 965–993.
[22] P. Yang, H. J. Fan, *Adv. Mater. Technol.* **2020**, *5*, 2000217.
[23] X. Li, B. Liu, B. Pei, J. Chen, D. Zhou, J. Peng, X. Zhang, W. Jia, T. Xu, *Chem. Rev.* **2020**, *120*, 10793–10833.
[24] Y. Sui, C. A. Zorman, *J. Electrochem. Soc.* **2020**, *167*, 037571.
[25] M. Singh, H. M. Haverinen, P. Dhagat, G. E. Jabbou, *Adv. Mater.* **2010**, *22*, 673–685.
[26] Y.-H. Suh, D.-W. Shin, Y. T. Chun, *RSC Adv.* **2019**, *9*, 38085.
[27] T. Xuan, S. Shi, L. Wang, H.-C. Kuo, R.-J. Xie, *J. Phys. Chem. Lett.* **2020**, *11*, 5184–5191.
[28] S. Chung, K. Cho, T. Lee, *Adv. Sci.* **2019**, *6*, 1801445.
[29] A. Sajedi-Moghaddam, E. Rahmanian, N. Naseri, *ACS Appl. Mater. Interfaces* **2020**, *12*, 34487–34504.
[30] F. C. Krebs, *Sol. Energy Mater.* **2009**, *93*, 465–475.
[31] S. Khan, L. Lorenzelli, R. S. Dahiya, *IEEE Sens. J.* **2015**, *15*, 3164–3185.
[32] H. W. Tan, *Virtual Physical Prototyping* **2016**, *11*, 271–288.
[33] I. Kim, S.-W. Kwak, K.-S. Kim, T.-M. Lee, J. Jo, J.-H. Kim, H.-J. Lee, *Microelectron. Eng.* **2012**, *98*, 587–589.
[34] M. Pudas, J. Hagberg, S. Leppävuori, *J. Eur. Ceram. Soc.* **2004**, *24*, 2943–2950.
[35] K. Arapov, E. Rubingh, R. Abbel, J. Laven, G. de With, H. Friedrich, *Adv. Funct. Mater.* **2016**, *26*, 586–593.
[36] K.-H. Shin, H. A. D. Nguyen, J. Park, D. Shin, D. Lee, *J. Coat. Technol. Res.* **2017**, *14*, 95–106.
[37] N. Lanigan, X. Wang, *Chem. Commun.* **2013**, *49*, 8133–8144.
[38] G. V. Oshovsky, D. N. Reinhoudt, W. Verboom, *Angew. Chem. Int. Ed.* **2007**, *46*, 2366–2393; *Angew. Chem.* **2007**, *119*, 2418–2445.
[39] P. Rosa, A. Câmara, C. Gouveia, *Open J. Internet of Things* **2015**, *1*, 16–36.
[40] P. V. Raje, N. C. Murmu, *Int. J. Emerging Technol. Adv. Eng.* **2014**, *4*, 174–183.
[41] J.-U. Park, M. Hardy, S. J. Kang, K. Barton, K. Adair, D. K. Mukhopadhyay, C. Y. Lee, M. S. Strano, A. G. Alleyne, J. G. Georgiadis, P. M. Ferreira, J. A. Rogers, *Nat. Mater.* **2007**, *6*, 782–789.
[42] S. Mishra, K. L. Barton, A. G. Alleyne, P. M. Ferreira, J. A. Rogers, *J. Micromech. Microeng.* **2010**, *20*, 095026.
[43] B. W. An, K. Kim, H. Lee, S.-Y. Kim, Y. Shim, D.-Y. Lee, J. Y. Song, J.-U. Park, *Adv. Mater.* **2015**, *27*, 4322–4328.
[44] H. K. Choi, J.-U. Park, O. O. Park, P. M. Ferreira, J. G. Georgiadis, J. A. Rogers, *Appl. Phys. Lett.* **2008**, *92*, 123109.
[45] J.-U. Park, J. H. Lee, U. Paik, Y. Lu, J. A. Rogers, *Nano Lett.* **2008**, *8*, 4210–4216.
[46] J.-U. Park, S. Lee, S. Unarunotai, Y. Sun, S. Dunham, T. Song, P. M. Ferreira, A. G. Alleyene, U. Paik, J. A. Rogers, *Nano Lett.* **2010**, *10*, 584–591.
[47] B. W. An, K. Kim, M. Kim, S.-Y. Kim, S.-H. Hur, J.-U. Park, *Small* **2015**, *11*, 2263–2268.
[48] K. Kim, G. Kim, B. R. Lee, S. Ji, S.-Y. Kim, B. W. An, M. H. Song, J.-U. Park, *Nanoscale* **2015**, *7*, 13410–13415.
[49] S. Jeong, J.-Y. Lee, S. S. Lee, Y.-H. Seo, S.-Y. Kim, J.-U. Park, B.-H. Ryu, W. Yang, J. Moon, Y. Choi, *J. Mater. Chem. C* **2013**, *1*, 4236–4243.
[50] "MicroFab printing system," can be found under http://www.microfab.com/printing-systems, **2021**.
[51] "Dimatix Materials Printer DMP-2850 | Fujifilm [United States]," can be found under https://www.fujifilm.com/us/en/business/inkjet-solutions/inkjet-technology-integration/dmp-2850, **2021**.

[52] "Ceradrop," can be found under http://www.ceradrop.com/en/, **2021**.
[53] "Microarray printing - microdrop Technologies," can be found under https://www.microdrop.de/microarray-printing.html, **2021**.
[54] H. Wijshoff, *Interface Sci.* **2018**, *36*, 20–27.
[55] J. E. Fromm, *IBM J. Res. Dev.* **1984**, *28*, 322–333.
[56] P.-G. de Gennes, F. Brochard-Wyart, D. Quéré, *Capillarity and Wetting Phenomena*, Springer, New York, **2004**.
[57] X. Zhang, J. Wang, L. Bao, E. Dietrich, R. C. A. van der Veen, S. Peng, J. Friend, H. J. W. Zandvliet, L. Yeo, D. Lohse, *Soft Matter* **2015**, *11*, 1889–1900.
[58] M. Parsa, S. Harmand, K. Se, *Adv. Colloid Interface Sci.* **2018**, *254*, 22–47.
[59] R. D. Deegan, O. Bakajin, T. F. Dupont, G. Huber, S. R. Nagel, T. A. Witten, **1997**, *389*, 827–829.
[60] N. Bridonneau, M. Zhao, N. Battaglini, G. Mattana, V. Thévenet, V. Noël, M. Roché, S. Zrig, F. Carn, *Langmuir* **2020**, *36*, 11411–11421.
[61] M. E. R. Shanahan, *Langmuir* **1995**, *11*, 1041–1043.
[62] D. I. Yu, H. J. Kwak, S. W. Doh, H. S. Ahn, H. S. Park, M. Kiyofumi, M. H. Kim, *Langmuir* **2015**, *31*, 1950–1957.
[63] L. Gao, T. J. McCarthy, *Langmuir* **2007**, *23*, 3762–3765.
[64] H. Y. Erbil, *Langmuir* **2020**, *36*, 2493–2509.
[65] H. Y. Erbil, *Surf. Sci. Rep.* **2014**, *69*, 325–365.
[66] M. He, D. Liao, H. Qiu, *Sci. Rep.* **2017**, *7*, 41897.
[67] J. Fan, J. De Coninck, H.-A. Wu, F.-C. Wang, *Phys. Rev. Lett.* **2020**, *124*, 125502.
[68] M. Kuang, L. Wang, Y. Song, *Adv. Mater.* **2014**, *26*, 6950–6958.
[69] J. Stringer, B. Derby, *Langmuir* **2010**, *26*, 10365–10372.
[70] P. C. Duineveld, *J. Fluid Mech.* **2003**, *477*, 175–200.
[71] V. Bromberg, S. Ma, T. J. Singler, *Appl. Phys. Lett.* **2013**, *102*, 214101.
[72] D. Kim, S. Jeong, B. K. Park, J. Moon, *Appl. Phys. Lett.* **2006**, *89*, 264101.
[73] D. Soltman, V. Subramanian, *Langmuir* **2008**, *24*, 2224–2231.
[74] B. Derby, *Annu. Rev. Mater. Res.* **2010**, *40*, 395–414.
[75] J. Stringer, T. M. Althagathi, C. C. W. Tse, V. D. Ta, J. D. Shephard, E. Esenturk, C. Connaughton, T. J. Wasley, J. Li, R. W. Kay, P. J. Smith, *Manuf. Rev.* **2016**, *3*, 12.
[76] L. R. Hart, J. L. Harries, B. W. Greenland, H. M. Colquhoun, W. Hayes, *ACS Appl. Mater. Interfaces* **2015**, *7*, 8906–8914.
[77] H. Li, J. Liu, K. Li, Y. Liu, *Sens. Actuators A* **2019**, *297*, 111552.
[78] K. Ozawa, T. Usui, K. Ide, H. Takahashi, S. Sakai, S. E. Corporation, *Soc. Imaging Sci. Technol.* **2007**, *2*, 898–901.
[79] C. N. Baroud, F. Gallaire, R. Dangla, *Lab Chip* **2010**, *10*, 2032–2045.
[80] I. Arango, L. Bonil, D. Posada, J. Arcila, *Int. J. Interact. Des. Manuf.* **2019**, *13*, 967–980.
[81] Y. Yonemoto, K. Tashiro, M. Yamashita, T. Kunugi, *Fluids* **2022**, *7*, 38.
[82] K.-S. Kwon, M. K. Rahman, T. H. Phung, S. Hoath, S. Jeong, J. S. Kim, *Flex. Print. Electron.* **2020**, *5*, 043003.
[83] K. Borchers, V. Schönhaar, T. Hirth, G. E. M. Tovar, A. Weber, *J. Dispersion Sci. Technol.* **2011**, *32*, 1759–1764.
[84] T.-H. Kang, S.-W. Lee, K. Hwang, W. Shim, K.-Y. Lee, J.-A. Lim, W.-R. Yu, I.-S. Choi, H. Yi, *ACS Appl. Mater. Interfaces* **2020**, *12*, 24231–24241.
[85] C. Lausted, T. Dahl, C. Warren, K. King, K. Smith, M. Johnson, R. Saleem, J. Aitchison, L. Hood, S. R. Lasky, *GenomeBiology* **2004**, *5*, R58.
[86] H. Li, Y. Huang, Z. Wei, W. Wang, Z. Yang, Z. Liang, Z. Li, *Sci. Rep.* **2019**, *9*, 5058.
[87] Y. H. Yun, B. K. Lee, J. S. Choi, S. Kim, B. Yoo, Y. S. Kim, K. Park, Y. W. Cho, *Anal. Sci.* **2011**, *27*, 375–379.
[88] M. Hou, H. Zhao, Y. Feng, J. Ge, *Bioresour. Bioprocess.* **2017**, *4*, 8.
[89] M. Tijero, R. Díez-Ahedo, F. Benito-Lopez, L. Basabe-Desmonts, V. Castro-López, A. Valero, *Biomicrofluidics* **2015**, *9*, 044124.
[90] H. M. Haverinen, R. A. Myllylä, G. E. Jabbour, *Appl. Phys. Lett.* **2009**, *94*, 073108.
[91] H. M. Haverinen, R. A. Myllyla, G. E. Jabbour, *J. Disp. Technol.* **2010**, *6*, 87–89.
[92] A. C. Small, J. H. Johnston, N. Clark, *Eur. J. Inorg. Chem.* **2010**, 242–247.
[93] D. Y. Kim, Y. J. Han, J. Choi, C. Sakong, B.-K. Ju, K. H. Cho, *Org. Electron.* **2020**, *84*, 105814.
[94] S. K. Gupta, M. F. Prodanov, W. Zhang, V. V. Vashchenko, T. Dudka, A. L. Rogach, A. K. Srivastava, *Nanoscale* **2019**, *11*, 20837–20846.
[95] H. Zhang, Q. Su, S. Chen, *Nat. Commun.* **2020**, *11*, 2826.
[96] G. Liu, L. Zhou, G. Zhang, Y. Li, L. Chai, Q. Fan, J. Shao, *Mater. Design* **2017**, *114*, 10–17.
[97] G. Liu, P. Han, Y. Wu, H. Li, L. Zhou, *Opt. Mater.* **2019**, *98*, 109503.
[98] V. O. Neterebskaia, A. O. Goncharenko, S. M. Morozova, D. S. Kolchanov, A. V. Vinogradov, *Nanomaterials* **2020**, *10*, 1538.
[99] W. Li, Y. Wang, M. Li, L. P. Garbarini, F. G. Omenetto, *Adv. Mater.* **2019**, *31*, 1901036.
[100] H. S. Kang, J. Lee, S. M. Cho, T. H. Park, M. J. Kim, C. Park, S. W. Lee, K. L. Kim, D. Y. Ryu, J. Huh, E. L. Thomas, C. Park, *Adv. Mater.* **2017**, *29*, 1700084.
[101] S. Y. Lee, G. Lee, D. Y. Kim, S. H. Jang, I. Choi, J. Park, H.-K. Park, J. W. Jung, K. H. Cho, J. Choi, *APL Photonics* **2021**, *6*, 056104.
[102] X. Peng, J. Yuan, S. Shen, M. Gao, A. S. R. Chesman, H. Yin, J. Cheng, Q. Zhang, D. Angmo, *Adv. Funct. Mater.* **2017**, *27*, 1703704.
[103] T. M. Eggenhuisen, Y. Galagan, A. F. K. V. Biezemans, T. M. W. L. Slaats, W. P. Voorthuijzen, S. Kommeren, S. Shanmugam, J. P. Teunissen, A. Hadipour, W. J. H. Verhees, S. C. Veenstra, M. J. J. Coenen, J. Gilot, R. Andriessen, W. A. Groen, *J. Mater. Chem. A* **2015**, *3*, 7255–7262.
[104] M. Orrill, S. LeBlanc, *J. Appl. Polym. Sci.* **2017**, *134*, 44256.
[105] O. Bubnova, Z. U. Khan, A. Malti, S. Braun, M. Fahlman, M. Berggren, X. Crispin, *Nat. Mater.* **2011**, *10*, 429–433.
[106] F. Jiao, C. Di, Y. Sun, P. Sheng, W. Xu, D. Zhu, *Philos. Trans. R. Soc. A* **2021**, *372*, 20130008.
[107] A. Besganz, V. Zöllmer, R. Kun, E. Pál, L. Walder, M. Busse, *Procedia Technol.* **2014**, *15*, 99–106.
[108] H. Andersson, P. Šuly, G. Thungström, M. Engholm, R. Zhang, J. Mašlík, H. Olin, *J. Low Power Electron. Appl.* **2019**, *9*, 14.
[109] H. Li, X. Fang, R. Li, B. Liu, H. Tang, X. Ding, Y. Xie, R. Zhou, G. Zhou, Y. Tang, *Nano Energy* **2020**, *78*, 105288.
[110] J. Lim, H. Jung, C. Baek, G.-T. Hwang, J. Ryu, D. Yoon, J. Yoo, K.-I. Park, J. H. Kim, *Nano Energy* **2017**, *41*, 337–343.
[111] M.-L. Seol, J.-W. Han, D.-I. Moon, K. J. Yoon, C. S. Hwang, M. Meyyappan, *Nano Energy* **2018**, *44*, 82–88.
[112] D. McManus, *Nat. Nanotechnol.* **2017**, *12*, 343–350.
[113] D. Nutting, J. F. Felix, E. Tillotson, D.-W. Shin, A. De Sanctis, H. Chang, N. Cole, S. Russo, A. Woodgate, I. Leontis, H. A. Fernández, M. F. Cracium, S. J. Haigh, F. Withers, *Nat. Commun.* **2020**, *11*, 3047.
[114] D. Mampallil, H. B. Eral, *Adv. Colloid Interface Sci.* **2018**, *252*, 38–54.
[115] K. N. Al-Milaji, H. Zhao, *J. Phys. Chem. C* **2019**, *123*, 12029–12041.
[116] M. Kuang, J. Wang, B. Bao, F. Li, L. Wang, L. Jiang, Y. Song, *Adv. Opt. Mater.* **2014**, *2*, 34–38.

[117] J. Park, J. Moon, *Langmuir* **2006**, *22*, 3506–3513.
[118] M. Anyfantakis, Z. Geng, M. Morel, S. Rudiuk, D. Baigl, *Langmuir* **2015**, *31*, 4113–4120.
[119] Z. Du, H. Zhou, Y. Han, *Colloids Surf.* **2020**, *602*, 125111.
[120] M.-W. Wang, T.-Y. Liu, D.-C. Pang, J.-C. Hung, C.-C. Tseng, *Coatings Technol.* **2014**, *259*, 340–345.
[121] D.-H. Lee, K.-T. Lim, E.-K. Park, J.-M. Kim, Y.-S. Kim, *Microelectron. Eng.* **2013**, *111*, 242–246.
[122] E. L. Talbot, L. Yang, C. D. Bain, *ACS Appl. Mater. Interfaces* **2014**, *6*, 9572–9583.
[123] A. Gençer, J. V. Rie, S. Lombardo, K. Kang, W. Thielemans, *Biomacromolecules* **2018**, *19*, 3233–3243.
[124] H. Li, D. Buesen, R. Williams, J. Henig, S. Stapf, K. Mukherjee, E. Freier, W. Lubitz, M. Winkler, T. Happe, N. Plumeré, *Chem. Sci.* **2018**, *9*, 7596–7605.
[125] J. Shi, L. Yang, C. D. Bain, *ACS Appl. Mater. Interfaces* **2019**, *11*, 14275–14285.
[126] K. N. Al-Milaji, H. Zhao, *Adv. Mater. Interfaces* **2018**, *5*, 1701561.
[127] K. N. Al-Milaji, H. Zhao, *Langmuir* **2019**, *35*, 2209–2220.
[128] K. N. Al-Milaji, *J. Colloid Interface Sci.* **2018**, *529*, 234–242.
[129] T. Cuk, S. M. Troian, C. M. Hong, S. Wagner, *Appl. Phys. Lett.* **2014**, *77*, 2063–2065.
[130] M. Layani, M. Gruchko, O. Milo, I. Balberg, D. Azulay, S. Magdassi, *ACS Nano* **2009**, *3*, 3537–3542.
[131] Z. Zhang, X. Zhang, Z. Xin, M. Deng, Y. Wen, Y. Song, *Adv. Mater.* **2013**, *25*, 6714–6718.
[132] S. Ma, L. Liu, V. Bromberg, T. J. Singler, *ACS Appl. Mater. Interfaces* **2014**, *6*, 19494–19498.
[133] A. Shimoni, S. Azoubel, S. Magdassi, *Nanoscale* **2014**, *6*, 11084–11089.
[134] N. T. Dinh, E. Sowade, T. Blaudeck, S. Hermann, R. D. Rodriguez, D. R. T. Zahn, S. E. Schulz, R. R. Baumann, O. Kanoun, *Carbon* **2016**, *96*, 382–393.
[135] D. S. Eom, J. Chang, J. T. Han, H. Kim, K. Cho, *J. Phys. Chem. C* **2014**, *118*, 27081–27090.
[136] Z. Zhang, W. Zhu, *J. Mater. Chem. C* **2014**, *2*, 9587–9591.
[137] T.-Y. Chu, Z. Zhang, Y. Tao, *Adv. Mater. Technol.* **2018**, 1700321.
[138] V. Slabov, A. V. Vinogradov, A. V. Yakovlev, *J. Mater. Chem. C* **2018**, *6*, 5269–5277.
[139] N. Bridonneau, G. Mattana, V. Noel, S. Zrig, F. Carn, *J. Phys. Chem. Lett.* **2020**, *11*, 4559–4563.
[140] K. N. Al-Milaji, R. L. Hadimani, S. Gupta, V. K. Pecharsky, H. Zhao, *Sci. Rep.* **2019**, *9*, 16261.
[141] L. Jacot-Descombes, M. R. Gullo, V. J. Cadarso, M. Mastrangeli, O. Ergeneman, C. Peters, P. Fatio, M. A. Freidy, C. Hierold, B. J. Nelson, J. Brugger, *Micromachines* **2014**, *5*, 583–593.
[142] H. Song, J. Spencer, A. Jander, J. Nielsen, J. Stasiak, V. Kasperchik, *J. Appl. Phys.* **2014**, *115*, 17E308.
[143] W. Kamal, J.-D. Lin, S. J. Elston, T. Ali, A. A. Castrejón-Pita, S. M. Morris, *Adv. Mater. Interfaces* **2020**, *7*, 2000578.
[144] R. D. Deegan, *Phys. Rev. E* **2000**, *61*, 475–485.
[145] L. Liu, Y. Pei, S. Ma, X. Sun, T. J. Singler, *Adv. Eng. Mater.* **2020**, *22*, 1901351.
[146] Y. Chu, C. Qian, P. Chahal, C. Cao, *Adv. Sci.* **2019**, *6*, 1801653.
[147] D. Maddipatla, B. B. Narakathu, M. Atashbar, *Biosensors* **2020**, *10*, 199.
[148] S. Schlisske, M. Held, T. Rödlmeier, S. Menghi, K. Fuchs, M. Ruscello, A. J. Morfa, U. Lemmer, G. Hernandez-Sosa, *Langmuir* **2018**, *34*, 5964–5970.
[149] Y.-L. Kuo, F.-C. Kung, C.-L. Ko, A. Okino, T.-C. Chiang, J.-Y. Guo, S.-Y. Chen, *Thin Solid Films* **2020**, *709*, 138152.
[150] O. Neděla, P. Slepička, Z. Kolská, N. Slepičková Kasálková, P. Sajdl, M. Veselý, V. Švorčík, *React. Funct. Polym.* **2016**, *100*, 44–52.
[151] A. Grandoni, G. Mannini, A. Glisenti, A. Manariti, *Appl. Surf. Sci.* **2017**, *420*, 579–585.
[152] V. Oliveira, R. Vilar, *Microsc. Microanal.* **2008**, *14*, 73–76.
[153] P. Bryk, E. Korczeniewski, G. S. Szymański, P. Kowalczyk, K. Terpiłowski, A. P. Terzyk, *Materials* **2020**, *13*, 1554.
[154] A. U. Alam, M. M. R. Howlader, M. J. Deen, *J. Micromech. Microeng.* **2014**, *24*, 035010.
[155] D. Tian, Y. Song, L. Jiang, *Chem. Soc. Rev.* **2013**, *42*, 5184.
[156] J.-S. Kwon, D. J. Lee, J. H. Oh, *Appl. Sci.* **2018**, *8*, 280.
[157] R. O. F. Verkuijlen, M. H. A. van Dongen, A. A. E. Stevens, J. van Geldrop, J. P. C. Bernards, *Appl. Surf. Sci.* **2014**, *290*, 381–387.
[158] B. J. Kang, Y. S. Kim, Y. W. Cho, J. H. Oh, *Microelectron. Eng.* **2011**, *88*, 2355–2358.
[159] T.-Y. Lin, T. T. Pfeiffer, P. B. Lillehoj, *RSC Adv.* **2017**, *7*, 37374–37379.
[160] T. Schmaltz, G. Sforazzini, T. Reichert, H. Frauenrath, *Adv. Mater.* **2017**, *29*, 1605286.
[161] S. Wu, Q. Zhang, Z. Chen, L. Mo, S. Shao, Z. Cui, *J. Mater. Chem. C* **2017**, *5*, 7495–7503.
[162] L. P. Yeo, B. K. Lok, Q. M. P. Nguyen, C. W. Lu, Y. C. Lam, *Int. J. Adv. Manuf. Technol.* **2014**, *71*, 1749–1755.
[163] P. Q. M. Nguyen, L.-P. Yeo, B.-K. Lok, Y.-C. Lam, *ACS Appl. Mater. Interfaces* **2014**, *6*, 4011–4016.
[164] Y. Tsuchiya, S. Haraguchi, M. Ogawa, T. Shiraki, H. Kakimoto, O. Gotou, T. Yamada, K. Okumoto, S. Nakatani, K. Sakanoue, S. Shinkai, *Adv. Mater.* **2012**, *24*, 968–972.
[165] S.-H. Lee, K.-Y. Shin, J. Y. Hwang, K. T. Kang, H. S. Kang, *J. Micromech. Microeng.* **2008**, *18*, 075014.
[166] H. Kim, G.-Y. Yun, S.-H. Lee, J.-M. Kim, *Sens. Actuators A* **2015**, *224*, 1–5.
[167] J. Z. Wang, Z. H. Zheng, H. W. Li, W. T. S. Huck, H. Sirringhaus, *Nat. Mater.* **2004**, *3*, 171–176.
[168] C. E. Hendriks, P. J. Smith, J. Perelaer, *Adv. Funct. Mater.* **2008**, *18*, 1031–1038.
[169] C.-M. Keum, I.-H. Lee, H.-L. Park, C. Kim, B. Lüssem, J. S. Choi, S.-D. Lee, *J. Appl. Phys.* **2017**, *121*, 244902.
[170] Z. Chen, F. Li, Q. Zeng, K. Yang, Y. Liu, Z. Su, G. Shan, *Org. Electron.* **2019**, *69*, 336–342.
[171] Y. Liu, F. Li, Z. Xu, C. Zheng, T. Guo, X. Xie, L. Qian, D. Fu, X. Yan, *ACS Appl. Mater. Interfaces* **2017**, *9*, 25506–25512.
[172] M. Pack, H. Hu, D.-O. Kim, X. Yang, Y. Sun, *Langmuir* **2015**, *31*, 7953–7961.
[173] P. Gao, A. Hunter, M. J. Summe, W. A. Phillip, *ACS Appl. Mater. Interfaces* **2016**, *8*, 19772–19779.
[174] P. Gao, A. Hunter, S. Benavides, M. J. Summe, F. Gao, W. A. Phillip, *ACS Appl. Mater. Interfaces* **2016**, *8*, 3386–3395.
[175] W. J. Hyun, E. B. Secor, C.-H. Kim, M. C. Hersam, L. F. Francis, C. D. Frisbie, *Adv. Energy Mater.* **2017**, *7*, 1700285.
[176] W. J. Hyun, E. B. Secor, F. Z. Bidoky, S. B. Walker, J. A. Lewis, M. C. Hersam, L. F. Francis, C. D. Frisbie, *Flex. Print. Electron.* **2018**, *3*, 035004.
[177] A. Mahajan, W. J. Hyun, S. B. Walker, G. A. Rojas, J.-H. Choi, J. A. Lewis, L. F. Francis, C. D. Frisbie, *Adv. Electron. Mater.* **2015**, *1*, 1500137.
[178] P. Maisch, L. M. Eisenhofer, K. C. Tam, A. Distler, M. M. Voigt, C. J. Brabec, H. J. Egelhaaf, *J. Mater. Chem. A* **2019**, *7*, 13215–13224.
[179] R. Raj, R. Enright, Y. Zhu, S. Adera, E. N. Wang, *Langmuir* **2012**, *28*, 15777–15788.
[180] R. Raj, S. Adera, R. Enright, E. N. Wang, *Nat. Commun.* **2014**, *5*, 4975.

[181] H.-Y. Tseng, V. Subramanian, *Org. Electron.* **2011**, *12*, 249–256.
[182] Y. Li, L. Lan, P. Xiao, S. Sun, Z. Lin, W. Song, E. Song, P. Gao, W. Wu, J. Peng, *ACS Appl. Mater. Interfaces* **2016**, *8*, 19643–19648.
[183] M. Mirbagheri, D. K. Hwang, *Adv. Mater. Interfaces* **2019**, *6*, 1970104.
[184] L. Challier, J. Lemarchand, C. Deanno, C. Jauzein, G. Mattana, G. Mériguet, B. Rotenberg, V. Noël, *Part. Part. Syst. Charact.* **2021**, *38*, 2000235.
[185] S. A. Elrod, B. Hadimioglu, B. T. Khuri-Yakub, E. G. Rawson, E. Richley, C. F. Quate, N. N. Mansour, T. S. Lundgren, *J. Appl. Phys.* **1989**, *65*, 3441.
[186] E. Sowade, K. Y. Mitra, E. Ramon, C. Martinez-Domingo, F. Villani, F. Loffredo, H. L. Gomes, R. R. Baumann, *Org. Electron.* **2016**, *30*, 237–246.
[187] K. Y. Mitra, E. Sowade, C. Martínez-Domingo, E. Ramon, J. Carrabina, H. L. Gomes, R. R. Baumann, *AIP Conf. Proc.* **2015**, *1646*, 106–114.
[188] M. Abulikemu, E. H. Da, M. A. Malik, G. E. Jabbour, *Angew. Chem.* **2014**, *126*, 430–433.
[189] S. I. Ahn, W. K. Kim, S. H. Ryu, K. J. Kim, S. E. Lee, S.-H. Kim, J.-C. Park, K. C. Choi, *Org. Electron.* **2012**, *13*, 980–984.
[190] M. Y. Teo, L. Stuart, H. Devaraj, C. Y. Liu, K. C. Aw, J. Stringer, *J. Mater. Chem. C* **2019**, *7*, 2219.
[191] M. Y. Teo, N. RaviChandran, N. Kim, S. Kee, L. Stuart, K. C. Aw, J. Stringer, *ACS Appl. Mater. Interfaces* **2019**, *11*, 37069–37076.
[192] F. Ge, X. Wang, Y. Zhang, E. Song, G. Zhang, H. Lu, K. Cho, L. Qiu, *Adv. Electron. Mater.* **2017**, *3*, 1600402.
[193] T. Çaykara, M. G. Sande, N. Azoia, L. R. Rodrigues, C. J. Silva, *Med. Microbiol. Immunol.* **2020**, *209*, 363–372.
[194] B. Lepoittevin, L. Costa, S. Pardoue, D. Dragoé, S. Mazerat, P. Roger, *Polym. Sci.* **2016**, *54*, 2689–2697.
[195] B. M. A. Meslmani, G. F. Mahmoud, T. Leichtweiß, B. Strehlow, F. O. Sommer, M. D. Lohoff, U. Bakowsky, *Mater. Sci. Eng. C* **2016**, *58*, 78–87.
[196] H. Salmi-Mani, G. Terreros, N. Barroca-Aubry, C. Aymes-Chodur, C. Regeard, P. Roger, *Eur. Polym. J.* **2018**, *103*, 51–58.
[197] J. Pinson, D. Thiry, Eds., in *Surface Modification of Polymers*, Wiley-VCH, Weinheim, **2019**.
[198] D. Hetemi, F. I. Podvorica, *Langmuir* **2016**, *32*, 512–518.
[199] A. Garcia, N. Hanifi, B. Jousselme, P. Jégou, S. Palacin, P. Viel, T. Berthelot, *Adv. Funct. Mater.* **2013**, *23*, 3668–3674.
[200] S. Vural, T. Seckin, *Adv. Polym. Technol.* **2018**, *37*, 1703–1711.
[201] T.-J. Liu, C.-H. Chen, P.-Y. Wu, C.-H. Lin, C.-M. Chen, *Langmuir* **2019**, *35*, 7212–7221.
[202] D. Li, L. Xu, J. Wang, J. E. Gautrot, *Adv. Healthcare Mater.* **2021**, *10*, 2000953.
[203] B. Lin, *Appl. Surf. Sci.* **2015**, *359*, 380–387.
[204] B. Yan, X. Zheng, P. Tang, H. Yang, J. He, S. Zhou, *ACS Appl. Mater. Interfaces* **2018**, *10*, 36249–36258.
[205] D. Chen, T. Wang, G. Song, Y. Du, J. Lv, X. Zhang, Y. Li, L. Zhang, J. Hu, Y. Fu, R. Jordan, *ACS Appl. Mater. Interfaces* **2019**, *11*, 41668–41675.
[206] T. Ding, C. Rüttiger, X. Zheng, F. Benz, H. Ohadi, G. A. E. Vandenbosch, V. V. Moshchalkov, M. Gallei, J. J. Baumberg, *Adv. Opt. Mater.* **2016**, *4*, 877–882.
[207] L. Zou, C. J. Addonizio, B. Su, M. J. Sis, A. S. Braegelman, D. Liu, M. J. Webber, *Biomacromolecules* **2021**, *22*, 171–182.
[208] L. Zou, M. J. Webber, *Chem. Commun.* **2019**, *55*, 9931.
[209] C. Yu, J. Schimelman, P. Wang, K. L. Miller, X. Ma, S. You, J. Guan, B. Sun, W. Zhu, S. Chen, *Chem. Rev.* **2020**, *120*, 10695–10743.
[210] X.-Y. Yu, J.-R. Chen, W.-J. Xiao, *Chem. Rev.* **2021**, *121*, 506–561.
[211] Y.-N. Zhou, J.-J. Li, Y.-Y. Wu, Z.-H. Luo, *Chem. Rev.* **2020**, *120*, 2950–3048.
[212] D. Roy, M. Semsarilar, J. T. Guthrie, *Chem. Soc. Rev.* **2009**, *38*, 2046–2064.
[213] S. Li, S. Zhang, X. Wang, *Langmuir* **2008**, *24*, 5585–5590.
[214] K. Yamada, T. G. Henares, K. Suzuki, D. Citterio, *Angew. Chem. Int. Ed.* **2015**, *54*, 5294–5310; *Angew. Chem.* **2015**, *127*, 5384–5401.
[215] D. Zhao, Y. Zhu, W. Cheng, W. Chen, Y. Wu, H. Yu, *Adv. Mater.* **2021**, *33*, 2000619.
[216] S. D. Hoath, Ed., *Fundamentals of Inkjet Printing: The Science of Inkjet and Droplets*, Wiley-VCH, Weinheim, **2016**.
[217] A. Zucca, C. Cipriani, S. Tarantino, D. Ricci, V. Mattoli, F. Greco, *Adv. Healthcare Mater.* **2015**, *4*, 983–990.
[218] V. Sanchez-Romaguera, S. Wunscher, B. M. Turki, R. Abbel, S. Barbosa, D. J. Tate, D. Oyeka, J. C. Batchelor, E. A. Parker, U. S. Schubert, S. G. Yeates, *J. Mater. Chem. C* **2015**, *3*, 2132.
[219] P. Li, H. P. A. Ali, W. Cheng, J. Yang, B. C. K. Tee, *Adv. Mater. Technol.* **2020**, *5*, 1900856.
[220] I. Bernacka-Wojcik, M. Huerta, K. Tybrandt, M. Karady, M. Y. Mulla, D. J. Poxson, E. O. Gabrielsson, K. Ljung, D. T. Simon, M. Berggren, E. Stavrinidou, *Small* **2019**, *15*, 1902189.
[221] W. Ait-Mammar, S. Zrig, N. Bridonneau, V. Noël, E. Stavrinidou, B. Piro, G. Mattana, *MRS Adv.* **2020**, *5*, 965–973.
[222] B. Piro, G. Mattana, V. Noël, *Sensors* **2019**, *19*, 4376.

Manuscript received: January 5, 2022
Accepted manuscript online: March 4, 2022
Version of record online: ■■, ■■

Reviews

Inkjet Printing

J. Lemarchand, N. Bridonneau, N. Battaglini, F. Carn, G. Mattana, B. Piro, S. Zrig, V. Noël* _____ e202200166

Challenges, Prospects, and Emerging Applications of Inkjet-Printed Electronics: A Chemist's Point of View

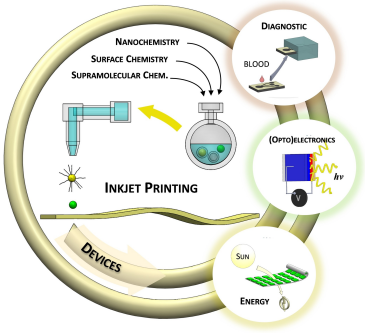

We focus on the field at the junction of inkjet printing and high-tech applications in optoelectronics, energy production and storage, and (bio)detection. We assess the micro- and nanostructuring inkjet printing methods and answer the following questions: What are the current, strategies to improve the resolution of printed patterns? To what extent can advances in nanochemistry, supramolecular chemistry, and surface chemistry be integrated into printing strategies?